Nuclear Physics B321 (1989) 1–38
North-Holland, Amsterdam

PROSPECTS FOR THE MEASUREMENT OF B_s^0–$\bar{B}_s^0$ MIXING

P. KRAWCZYK*, D. LONDON and H. STEGER

Deutsches Elektronen Synchrotron – DESY, Hamburg, Fed. Rep. Germany

Received 23 November 1988

We critically examine various experimental methods for determining the mixing parameter x_s in the B_s system, particularly for the case $x_s \geqslant 3$, as predicted in the standard model. Both the possibility of direct observation of time dependent oscillations and the use of time integrated methods are discussed. We find that time integrated methods are not likely to be able to measure x_s with sufficient accuracy to further restrict its value. Time dependent techniques are therefore necessary. For an asymmetric e^+e^- collider running near the $\Upsilon(5S)$, such a measurement is sensitive to values of x_s up to about 10, with 5×10^6 $b\bar{b}$ quark pairs required. For conventional machines running at energies high above the $B_s^0\bar{B}_s^0$ threshold, at least 3×10^8 $b\bar{b}$'s are necessary, but x_s up to 15 is accessible.

1. Introduction

The recent observation of B_d^0–$\bar{B}_d^0$ mixing by ARGUS [1] (and the subsequent confirmation by CLEO [2]) has far reaching consequences. In the three family standard model, its unexpectedly large magnitude implies, for example, an increased lower bound on the top quark mass [3] and, at the same time leads to improved bounds on the Cabibbo–Kobayashi–Maskawa (CKM) matrix elements [4]. Another consequence of this experimental result is a lower limit on the mixing parameter $x_s = \Delta M_{B_s}/\Gamma_{B_s}$ for the $B_s^0\bar{B}_s^0$ system, predicted to be $x_s \geqslant 3$ [5]. The measurement of x_s is therefore of immediate interest. Should x_s be found to be less than 3, this would be a spectacular indication of new physics. On the other hand, a precise determination of x_s within the standard model range would be of equal importance, especially if m_t were known. In this case, the *CP* violating phase of the CKM matrix would become tightly constrained.

The importance of b physics has been realized and will be studied with the use of accelerators presently under construction or in the planning stage. b quarks are copiously produced in e^+e^- collisions at the Υ or the Z^0 resonance. In particular, with its designed luminosity, 10^6 $b\bar{b}$ pairs per year are expected at LEP [6], and about 10^5 at SLC [7]. Dedicated machines, such as the one planned at PSI, would

* Alexander Von Humboldt fellow. On leave of absence from the Institute of Theoretical Physics, Warsaw University, Warsaw, Poland.

0550-3213/89/$03.50

even reach 10^7 $b\bar{b}$ pairs per year [8]. The ep collider HERA, with about 10^6 $b\bar{b}$'s predicted [9], will also be a useful tool for studying heavy flavour physics. Finally, hadron colliders (TeVatron, SSC) and fixed target machines (TeVatron, UNK) can provide much larger numbers of $b\bar{b}$ pairs, which, however, must be separated from an enormous background.

In this paper we discuss various methods for obtaining the quantity x_s experimentally. For each method, there are several considerations. The accuracy with which the relevant observables must be measured in order to give further constraints on the standard model parameters is determined. We also present the range of x_s to which each method is sensitive. Finally, the number of $b\bar{b}$ quark pairs required for such a measurement is estimated. In sect. 2 we survey experimental methods utilizing time integrated probabilities of particle–antiparticle transitions. After a brief presentation of the observables involved and the accuracy requirements (subsect. 2.1), we consider experiments which measure the ratio of same sign to opposite sign dilepton production rates at the Υ(5S) resonance (subsect. 2.2). In subsect. 2.3 we extend our investigation, considering dilepton events with an additional D_s tag. The oscillations of B_s mesons produced at energies high above threshold are discussed in subsect. 2.4. In sect. 3 we examine the prospects for direct observation of time dependent B_s–$\bar{B}_s$ oscillations. We first consider an experimental situation involving B_s mesons produced at high energies (subsect. 3.1). It is also possible to measure x_s via time dependent means when the CM energy is near the Υ(5S) mass. This is discussed in subsect. 3.2. Our conclusions are presented in sect. 4.

2. Time integrated methods

2.1. OBSERVABLES AND ACCURACY REQUIREMENTS

Time integrated methods always measure certain probability ratios [10]. The dependence of these ratios on the mixing parameter, x_q, is determined by the initial state. Since b quarks are produced in pairs, we can distinguish between the following two situations. In the first case, one of the b's hadronizes into a neutral B_q^0 or $\bar{B}_q^0$ meson, while the other goes into a different kind of B particle (e.g. $B^{\pm}$, Λ_b, etc.) which can be used as a tag to obtain the b quantum number of the B_q. We will refer to this as a "single particle initial state" for the rest of this section. In this case, the time integrated methods determine the following two quantities of interest [11]:

$$r_q \equiv \frac{P\left(B_q^0 \to \bar{B}_q^0\right)}{P\left(B_q^0 \to B_q^0\right)}, \tag{1a}$$

$$\bar{r}_q \equiv \frac{P\left(\bar{B}_q^0 \to B_q^0\right)}{P\left(\bar{B}_q^0 \to \bar{B}_q^0\right)}. \tag{1b}$$

In the standard model one finds [12] that $r \simeq \bar{r}$ (ignoring CP violation) for both B_d and B_s mesons and that these quantities are related to x_q by

$$r_q \simeq \bar{r}_q \simeq \frac{x_q^2}{2 + x_q^2}, \tag{2}$$

where we have neglected the difference in widths between the two B's [12]. In the second case the two b's hadronize into a $B_q^0\bar{B}_q^0$ pair (we will refer to this as a "two particle initial state"). This situation is more complicated. The $B_q^0\bar{B}_q^0$ system can be produced either in a pure quantum state with definite angular momentum L, or in a mixed state. Close to threshold, the $B_q^0\bar{B}_q^0$ pair is produced in an L odd configuration (as, for instance, in $\Upsilon(4S) \to B_d^0\bar{B}_d^0$). As the energy increases, one can also produce radial excitations of B_q ($\bar{B}_q$) giving rise to L even configurations via photon emission: $B_q^*\bar{B}_q$ ($B_q\bar{B}_q^*$) $\to \gamma B_q\bar{B}_q$. At much higher energies the B_q mesons are produced in association with other particles and therefore constitute an incoherent mixture. The relevant quantity, which can be related to experimental data in each case, is the ratio

$$R_q = \frac{P\left(B_q^0\bar{B}_q^0 \to B_q^0B_q^0\right) + P\left(B_q^0\bar{B}_q^0 \to \bar{B}_q^0\bar{B}_q^0\right)}{P\left(B_q^0\bar{B}_q^0 \to B_q^0\bar{B}_q^0\right)}. \tag{3}$$

In the standard model, one finds:

$$R_q^{\mathrm{o}} \simeq r_q \simeq \frac{x_q^2}{2 + x_q^2} \overset{x_q \text{ large}}{\simeq} 1 - \frac{2}{x_q^2}, \tag{4a}$$

$$R_q^{\mathrm{e}} \simeq \frac{3x_q^2 + x_q^4}{2 + x_q^2 + x_q^4} \overset{x_q \text{ large}}{\simeq} 1 + \frac{2}{x_q^2}, \tag{4b}$$

$$R_q^{\mathrm{inc}} = \left(\frac{R^{\mathrm{e}}}{R^{\mathrm{e}} + 1} + \frac{R^{\mathrm{o}}}{R^{\mathrm{o}} + 1}\right) \Bigg/ \left(\frac{1}{R^{\mathrm{e}} + 1} + \frac{1}{R^{\mathrm{o}} + 1}\right)$$

$$\simeq \frac{2r_q}{1 + r_q^2} \simeq \frac{2x_q^2 + x_q^4}{2 + 2x_q^2 + x_q^4} \overset{x_q \text{ large}}{\simeq} 1 - \frac{2}{x_q^4}, \tag{4c}$$

where R_q^{o}, R_q^{e}, and R_q^{inc} correspond to the $B_q^0\bar{B}_q^0$ pair being produced in odd, even, and incoherent states of angular momentum, respectively.

Within the standard model one expects the following relation to hold:

$$\frac{x_s}{x_d} = \left| \frac{V_{ts}}{V_{td}} \right|^2 \cdot (1+\delta), \tag{5}$$

where V_{ts} and V_{td} are CKM matrix elements, and δ comprises the SU(3) breaking corrections. Using the measured value of x_d (combining the results of ARGUS [1] and CLEO [2]),

$$x_d = 0.70 \pm 0.13, \tag{6}$$

and available information on the mixing matrix, one finds as a conservative lower bound [5]:

$$x_s \geqslant 3. \tag{7}$$

Since the mixing is expected to be large, it is clear from eqs. (2) and (4) that the time integrated observables are rather insensitive to x_s, and have to be determined to high precision in order to give useful information. For B_s, for the values of x_s expected in the standard model (eq. (7)), the error on x is much larger in the case where $B\bar{B}$ pairs are produced in an incoherent state of angular momentum (eq. (4c)) than when they are produced with L even or L odd (eqs. (4a, b)). This can be seen explicitly from the dependence of the error Δx on x, R, and ΔR (the experimental error on R):

$$\frac{\Delta x}{x} \simeq \begin{cases} \left(\dfrac{x^2}{4}\right)\dfrac{\Delta R}{R}, & L \text{ even, } L \text{ odd, single-particle,} \\[2ex] \left(\dfrac{x^4}{8}\right)\dfrac{\Delta R}{R}, & \text{incoherent mixture of } L. \end{cases} \tag{8}$$

Therefore, time integrated measurements are best done for the single particle initial state, or when the two particle initial state has a definite L, and we shall concentrate on such cases. As is clear from eq. (4), a value for x_s within the allowed region leads to a value for the observables which is close to 1, that is, $|1-R| \ll 1$, with $R = r$, R^o, or R^e. In any given experimental situation the accuracy needed to test the standard model depends on the actual value of the measured observable. However, an accuracy better than $|1-R|/2$ will always further constrain the parameter space. In particular, the minimal allowed value $x_3 = 3$ implies $|1-R_s| = 0.18$. Therefore, in order to further constrain the allowed range of x_s, *we require that* R_s *be measured to an accuracy of order* 10% *or better*. We will take this point as the basis of our further considerations.

2.2. TWO PARTICLE INITIAL STATES (1): DILEPTONS

We begin our discussion with the method which is most likely to be used in the near future, and which was successfully used by ARGUS and CLEO to obtain x_d. This consists of measuring the ratio of same sign to opposite sign dilepton production rates. Let us remark that, because of the reasons mentioned in the previous subsection, such an experiment cannot be performed in an environment where the $B\bar{B}$ pair is produced in an incoherent state of angular momentum. This excludes, for example, the use of B's produced at the Z^0 resonance. On the other hand, the resonance $\Upsilon(5S)$ is an obvious candidate source for $B_s^0\bar{B}_s^0$ pairs with definite angular momentum. The situation here, however, is much more complicated than at the $\Upsilon(4S)$ resonance.

The experimentally determined ratio R_{exp} of same sign to opposite sign dileptons is not equal to any one of the quantities R_q^L introduced in eq. (4), because of a variety of contributing modes.

(i) $B_q^0\bar{B}_q^0$

One of the main difficulties in extracting the value of x_s is due to the fact that both B_d and B_s mesons in odd and even angular momentum states contribute to R_{exp}. Since the mass splitting between B_s and B_d is expected to be close to the D_s–D mass difference, and since the hyperfine splitting in the B_s system is likely to be similar to that in the B_d system, we will take

$$\Delta m_{B_s - B_d} \simeq 100 \text{ MeV}, \qquad \Delta m_{B_s^* - B_s} \simeq 50 \text{ MeV}. \tag{9}$$

Therefore, $B_s\bar{B}_s$ pairs are always accompanied by $B_d\bar{B}_d$, $B_d\bar{B}_d^*$, $B_d^*\bar{B}_d$ and $B_d^*\bar{B}_d^*$ pairs. Since the mass of the $\Upsilon(5S)$ is 310 MeV + $2m_{B_d}$, pairs of $B_s\bar{B}_s^*$ ($B_s^*\bar{B}_s$) are also expected to be produced. However, it is unclear whether $B_s^*\bar{B}_s^*$ can be produced. In any case there are four different modes contributing to the lepton rate: $B_d^0\bar{B}_d^0$ pairs in odd or even angular momentum states, and $B_s^0\bar{B}_s^0$ pairs with L odd or even.

(ii) B^+B^-

As at the $\Upsilon(4S)$, there is the contribution of charged B^+B^- pairs to the opposite sign dileptons. Its weight relative to that due to $B_d^0\bar{B}_d^0$ pairs is given by the quantity λ which is a straightforward generalization of the one used by ARGUS [1]:

$$\lambda = \frac{\mathrm{Br}(\Upsilon \to B^+B^-)}{\mathrm{Br}(\Upsilon \to B_d^0\bar{B}_d^0)}, \tag{10}$$

where we have assumed equal semileptonic branching ratios for B_d^0 and B^+ decays. In eq. (10), radial excitations, both in the numerator and denominator, are understood to be included in the quantity λ, which is estimated to be in the range 1–1.5. (For a review of the theory of $B\bar{B}$ mixing, see ref. [10].)

(iii) $B\bar{B}\pi$

Another factor which must be taken into account is due to the production of BB pairs in association with a pion, e.g. $B_d^0\bar{B}_d^0\pi^0$, $B^+B^-\pi^0$, $B^+\pi^-\bar{B}_d^0$, $B_d^*\bar{B}_d\pi^0$, etc. In analogy to eq. (10) we parametrize this contribution as ρ, defined by

$$\rho \equiv \frac{\mathrm{Br}(\Upsilon \to B\bar{B}\pi)}{\mathrm{Br}(\Upsilon \to B_d\bar{B}_d)}, \tag{11}$$

where we have again assumed equal semi-leptonic branching ratios for B_d and B^+, and excited states are implicitly included in both numerator and denominator. It is possible to estimate the relative contributions of $B_d^0\bar{B}_d^0\pi^0$, $B^+B^-\pi^0$, and $B^+\pi^-\bar{B}_d^0$ to ρ as follows. First, in analogy to eq. (10), the ratio of $B^+B^-\pi^0$ production to $B_d^0\bar{B}_d^0\pi^0$ production is expected to be about λ. Secondly, due to isospin considerations, the contribution of $B_d^0\bar{B}_d^0\pi^0$ is four times smaller than that of $B^+\bar{B}_d^0\pi^- +$ c.c. Therefore we have

$$\begin{array}{ccccc} B^+B^-\pi^0 & : & B^+\bar{B}_d^0\pi^- + B^-B_d\pi^+ & : & B_d^0\bar{B}_d^0\pi^0 \\ \lambda & : & 4 & : & 1 \end{array}. \tag{12}$$

The combination $(\rho/\lambda)[4/(\rho+\lambda+5)]$ may be experimentally accessible via the measurement of the ratio of the production rates of singly charged B's and B^+B^- pairs at the $\Upsilon(5S)$. In the following we assume ρ to be 1 since, apart from phase space, there seems to be no indication that the production of an extra pion would be suppressed. We hope, however, that this assumption will be substantiated by experiment in the near future. We will see that the size of this background is important.

There is also likely to be a background contribution from the production of $B\bar{B}\pi\pi$ final states. We will disregard this in the following discussion. In principle, this can be treated in an analogous way to the $B\bar{B}\pi$ background. However, we do not expect the two pion contribution to be large because of the limited phase space available. Furthermore, for reasons detailed below, it may be necessary to choose the CM energy of the collider to be below the $\Upsilon(5S)$, and this background may not even be present.

In order to take all these factors into account in the extraction of R_s from R_{exp}, it is convenient to introduce the quantity $\tilde{R}$:

$$\tilde{R} \equiv \left\{ \frac{N(\ell^+\ell^+) + N(\ell^-\ell^-)}{N(\ell^+\ell^-)} \right\}_{\text{only from } B^0\bar{B}^0}. \tag{13}$$

$\tilde{R}$ is related to $R_{\exp}$ by*

$$\tilde{R} = \left[((k+1)(\lambda+5) + \lambda(\rho+\lambda+5)) R_{\exp} + \tfrac{9}{2}\rho \frac{R_{\exp} - R_{d_o}}{1 + R_{d_o}} + \tfrac{1}{2}\rho \frac{R_{\exp} - R_{d_e}}{1 + R_{d_e}} \right]$$

$$\times \left[(k+1)(\lambda+5) - \lambda(\rho+\lambda+5) R_{\exp} - \tfrac{9}{2}\rho \frac{R_{\exp} - R_{d_o}}{1 + R_{d_o}} - \tfrac{1}{2}\rho \frac{R_{\exp} - R_{d_e}}{1 + R_{d_e}} \right]^{-1}, \tag{14}$$

where k is the ratio of $B_s\bar{B}_s$ to $B_d\bar{B}_d$ production rates, and λ and ρ have been defined above. The subscripts d_o and d_e refer to $B_d^0\bar{B}_d^0$ pairs with L odd and L even, respectively. In eq. (14), we have assumed that the $B_d^0\bar{B}_d^0$ pairs coming from the $B_d^0\bar{B}_0\pi^0$ background are produced in an incoherent state of angular momentum, i.e. they contribute equally to the d_o and d_e terms (the B_d^0's ($\bar{B}_d^0$'s) coming from $B^-B_d^0\pi^+$ ($B^+\bar{B}_d^0\pi^-$) contribute only to the d_o term). It is easy to see that $\tilde{R}$ is given by:

$$\tilde{R} = \left(\frac{\hat{d}_e}{1 + R_{d_e}} R_{d_e} + \frac{\hat{d}_o}{1 + R_{d_o}} R_{d_o} + \frac{\hat{s}_e}{1 + R_{s_e}} R_{s_e} + \frac{\hat{s}_o}{1 + R_{s_o}} R_{s_o} \right)$$

$$\times \left(\frac{\hat{d}_e}{1 + R_{d_e}} + \frac{\hat{d}_o}{1 + R_{d_o}} + \frac{\hat{s}_e}{1 + R_{s_e}} + \frac{\hat{s}_o}{1 + R_{s_o}} \right)^{-1}. \tag{15}$$

Again, the subscripts above refer to the $B\bar{B}$ modes of the respective type. In eq. (15), $\hat{d}_e$ denotes:

$$\hat{d}_e \equiv \frac{N(B_d^0\bar{B}_d^0,\, L \text{ even})}{N(B^0\bar{B}^0)_{\text{total}}} \cdot \left[\text{Br}(B_d^0 \to \ell^+ X) \right]^2, \tag{16}$$

with analogous definitions for $\hat{d}_o$, $\hat{s}_e$, and $\hat{s}_o$. Assuming the semileptonic branching ratios for B_d and B_s decays to be the same, one finds

$$\hat{d}_e + \hat{d}_o + \hat{s}_e + \hat{s}_o = \left[\text{Br}(B_{d,s}^0 \to \ell^+ X \right]^2. \tag{17}$$

It follows from eq. (15) that $\tilde{R}$ is extremely sensitive to the ratio of the production rates of B_s mesons in L even and L odd states. If these production rates are equal, this is equivalent to producing B_s mesons in an incoherent state of

* Following ARGUS we assume that the background contribution to the same sign dileptons coming from charm decays can be determined, and is small for appropriate cuts imposed on the lepton energies. However, these cuts eliminate about half the signal as well.

TABLE 1

Ratios of probabilities for the decay of $\Upsilon(5s)$ into various states, for two potential model calculations. In the first line, the mass of the $\Upsilon(5s)$ is assumed to be smaller than $2m_{B_s^*}$; the last two lines assume that $B_s^*\bar{B}_s^*$ pairs can be produced.

	$B_d^*\bar{B}_d^*$	$B_s^*\bar{B}_s^*$	$B_d\bar{B}_d^*$ + c.c.	$B_s\bar{B}_s^*$ + c.c.	$B_d\bar{B}_d$	$B_s\bar{B}_s$
BHI [13]	1	—	0.41	0.34	0.03	0.004
BHII [13]	1	0.67	0.41	0.18	0.03	0.004
CUSB [14]	1	1.18	1.34	0.1	0.67	0.21

angular momentum and, as can be seen from eqs. (4) and (8), this implies that the resulting error in x_s is too large. It is therefore very important to know how close to an incoherent state the actual situation is, i.e. to know the ratio $\hat{s}_o/\hat{s}_e$ rather well. Explicitly, for the combination of R_s's which enter eq. (15), we have

$$\frac{R_{s_e}}{1+R_{s_e}}\hat{s}_e + \frac{R_{s_o}}{1+R_{s_o}}\hat{s}_o = \tfrac{1}{2}\hat{s}_e\left[\left(1+\frac{\hat{s}_o}{\hat{s}_e}\right) + \left(1-\frac{\hat{s}_o}{\hat{s}_e}\right)\frac{1}{x_s^2} + O\left(\frac{1}{x_s^4}\right)\right],$$

$$\frac{1}{1+R_{s_e}}\hat{s}_e + \frac{1}{1+R_{s_o}}\hat{s}_o = \tfrac{1}{2}\hat{s}_e\left[\left(1+\frac{\hat{s}_o}{\hat{s}_e}\right) - \left(1-\frac{\hat{s}_o}{\hat{s}_e}\right)\frac{1}{x_s^2} + O\left(\frac{1}{x_s^4}\right)\right]. \qquad (18)$$

In principle one can calculate the relative production probabilities for the various modes using potential models [13–15] (which also include coupled channel analyses). However, as can be seen from table 1, there are considerable theoretical uncertainties involved. We are left, therefore, with three possibilities. The first is to experimentally determine this ratio. Unfortunately, there does not seem to be any easy way to do this. Furthermore, it is unlikely that $\hat{s}_o/\hat{s}_e$ could be obtained with sufficient accuracy to yield a 10% measurement of R_s. Another possibility is to run the experiment at the threshold for $B_s^0\bar{B}_s^0$ production (~ 10.8 GeV), thereby eliminating all higher excitations. However, as can be seen in fig. 1, in which the cross section for e^+–e^- annihilation into hadrons is plotted versus the center of mass energy [16], the cross section is substantially reduced at this energy. Finally, according to potential model calculations, it might be possible to tune the CM energy of the collider to a value such that one angular momentum state dominates over the other. For example, such a situation is predicted at the $\Upsilon(5S)$ resonance with $m_{\Upsilon(5S)} < 2m_{B_s^*}$ in the scenario presented in the first row of table 1 [13], for which one finds

$$\frac{\mathrm{Br}(\Upsilon \to B_s\bar{B}_s)}{\mathrm{Br}(\Upsilon \to B_s\bar{B}_s^* + \bar{B}_s B_s^*)} \simeq 10^{-2}, \qquad (19)$$

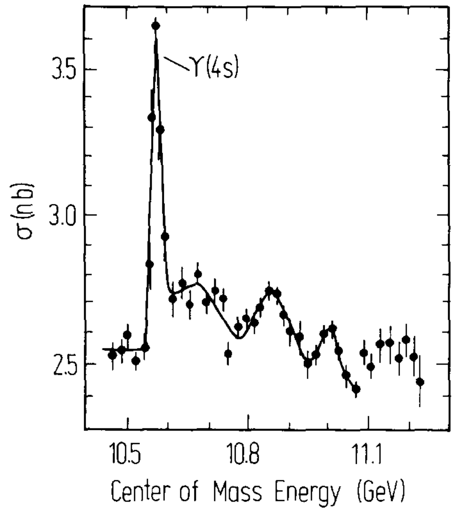

Fig. 1. The ratio $R = \sigma(e^+e^- \to \text{hadrons})/\sigma(e^+e^- \to \mu^+\mu^-)$ vs. centre of mass energy in the region of Υ resonances [16] (reprinted with permission).

i.e. $\hat{s}_o/\hat{s}_e \simeq 0$. This seems to be the only type of scenario in which R_s can be measured to the prescribed accuracy. Thus in what follows we shall neglect the L odd $B_s\bar{B}_s$ configuration altogether. (Should it turn out that $B_s^*\bar{B}_s^*$ pairs are produced at the $\Upsilon(5S)$ resonance, we suggest tuning the energy slightly below the peak. As can be seen from fig. 1, there is almost no loss in the $B\bar{B}$ production rate below the estimated $B_s^*\bar{B}_s^*$ threshold. It may also be that including $B_s^*\bar{B}_s^*$ pairs will yield a situation in which $\hat{s}_e/\hat{s}_o \simeq 0$. This is equally acceptable, and yields a similar analysis to that which follows.) We must emphasize that more theoretical work must be done to ascertain whether or not one angular momentum state dominates over the other. *Should this assumption turn out not to be realized, however, then this time integrated method for measuring x_s appears much less promising.*

We now address the question of whether or not the required accuracy in R_s can be achieved even under this assumption. Defining the parameters k and p by:

$$k = \frac{\hat{s}_e}{\hat{d}_e + \hat{d}_o}, \qquad p = \frac{\hat{d}_e}{\hat{d}_o}, \tag{20}$$

R_{s_e} can then be written as

$$R_{s_e} = \frac{k\tilde{R} + f}{k - f}, \tag{21}$$

where

$$f = f(p, \tilde{R}, x_d) \equiv \frac{1}{1+p}\left[p\frac{\tilde{R}-R_{d_e}}{1+R_{d_e}} + \frac{\tilde{R}-R_{d_o}}{1+R_{d_o}}\right]. \tag{22}$$

k is, in principle, experimentally accessible by measuring the K meson yield above and below the threshold for B_s production. However, not enough is known about kaon production in the decays of B_d and B_s mesons to reliably extract k from such a measurement. k can also be estimated using potential models (e.g. $k \simeq 0.25$ [13]). However, in light of the uncertainties of these models, we will, for the moment, keep it as a free parameter (although the range $0.2 \leqslant k \leqslant 0.5$ (continuum) seems reasonable). As for the parameter p, it may be possible to measure the ratio of the number of $B\bar{B}$ pairs in even-L states to the number in odd-L states by looking at the angular correlation between same sign dileptons [17]. This will determine p provided k is known. In view of the strikingly different values for p predicted by various models (see table 1), we regard it as a free parameter (varying in the range $0 \leqslant p < \infty$).

In order to estimate the (in)sensitivity of R_{s_e} to various quantities one has to calculate the respective derivatives. One easily finds, for instance

$$\frac{\partial R_{s_e}}{\partial k} = -\frac{1+R_s}{k(1+k)(1+p)}\left\{p\frac{R_{s_e}-R_{d_e}}{1+R_{d_e}} + \frac{R_{s_e}-R_{d_o}}{1+R_{d_o}}\right\}. \tag{23}$$

For the sake of a numerical estimate, we take $R_{s_e} = 1$, $x_d = 0.7$, $k = 0.25$, and consider the two extreme cases, $p = 0$ and $p \to \infty$. For the contribution of the uncertainty in k to the error in R_{s_e}, one gets

$$\left|\frac{\partial R_{s_e}}{\partial k}\right|\Delta k = \frac{\Delta k}{k(1+k)}\begin{cases}1.33, & \text{for } p = 0,\\ 0.42, & \text{for } p \to \infty,\end{cases}$$

$$= \Delta k\begin{cases}4.2,\\ 1.4,\end{cases} \quad \text{for } k = 0.25. \tag{24a}$$

The other contributions to the error can be calculated similarly:

$$\left|\frac{\partial R_{s_e}}{\partial f}\right|\Delta f_p = \Delta f_p\begin{cases}12.2,\\ 9.3,\end{cases} \quad \text{for } k = 0.25, \tag{24b}$$

$$\left|\frac{\partial R_{s_e}}{\partial x_d}\right|\Delta x_d = \Delta x_d\begin{cases}5.0,\\ 8.2,\end{cases} \quad \text{for } k = 0.25, \tag{24c}$$

$$\left|\frac{\partial R_{s_e}}{\partial \tilde{R}}\right|\Delta \tilde{R} = \Delta \tilde{R}\begin{cases}11.7,\\ 6.7,\end{cases} \quad \text{for } k = 0.25, \tag{24d}$$

where Δf_p denotes the change in the function f when p varies between 0 and ∞:

$$\Delta f_p = \frac{2k}{5+3k} - \frac{k}{4.8k+5.8} = 0.05, \qquad \text{for } k = 0.25. \tag{25}$$

As a first remark we observe that the derivative of R_{s_e} with respect to $\tilde{R}$ is very large. This calls for an accuracy in $\tilde{R}$ to be better than 0.01. In view of the uncertainty in the values of λ and ρ, such a precision seems out of reach. We therefore conclude that the like sign dilepton quantities at the Υ(5S) cannot be used in this form to determine x_s if the standard model holds, even if k and p are known exactly. On the other hand, using $R_{s_e} \simeq 1$, measuring $\tilde{R}$ would give information on the parameters k and p:

$$\tilde{R} = \left[\frac{1}{1+p}\left(p\frac{R_{d_e}}{1+R_{d_e}} + \frac{R_{d_o}}{1+R_{d_o}}\right) + \tfrac{1}{2}k\right]\left[\frac{1}{1+p}\left(p\frac{1}{1+R_{d_e}} + \frac{1}{1+R_{d_o}}\right) + \tfrac{1}{2}k\right]^{-1}. \tag{26}$$

This should be of direct interest as a test for potential models.

The derivatives of R_s have the following important feature. In the limit of large k all but $\partial R_{s_e}/\partial\tilde{R}$ tend to zero. The asymptotic $1/k^2$ behaviour of $\partial R_{s_e}/\partial k$ implies that even if the uncertainty in k is of the same order as k itself, its contribution to $\Delta\tilde{R}$ still decreases like $1/k$. At the same time $\partial R_{s_e}/\partial\tilde{R}$ tends to 1. Therefore if one were able to effectively increase k, ΔR_{s_e} would be limited mainly by the experimental error on $\tilde{R}$. This will be discussed in the next section.

2.3. TWO PARTICLE INITIAL STATES (2): DILEPTONS WITH D_s TAG

The formalism introduced above applies equally well for a slightly modified experimental situation. In particular, putting additional constraints on the final state (beyond the existence of two leptons) results in changes in the effective values of k, p, λ and ρ. Such constraints can be used to enrich the sample in leptons originating from $B_s\bar{B}_s$ pairs, and thus allow one to reach the required 10% accuracy in R_s.

Perhaps the simplest way to achieve this goal is to tag on a D_s meson in addition to the dileptons. Although this will considerably enrich the ratio of B_s's to B_d's in the sample, there will still be some background. In this situation one finds

$$k_{\text{eff}} = \frac{\hat{s}_e}{\hat{d}_o + \hat{d}_e} \frac{\text{Br}(B_s \to \ell D_s X)}{\text{Br}(B_d \to \ell D_s X) \cdot \varepsilon}, \tag{27}$$

while the other parameters remain unchanged. Here, ε represents the experimental efficiency for rejecting the mode $B_d \to \ell D_s X$. Neither of the two semileptonic branching ratios used in eq. (27) is known. However, one can estimate them in the following way. Up to SU(3) flavour breaking corrections, one has $\mathrm{Br}(B_s \to \ell^+ D_s^- X) \simeq \mathrm{Br}(B_d \to \ell^+ D^- X)$. Using the experimental number [18]

$$\mathrm{Br}(B_d \to D^{*-} \ell^+ \nu) = (7.0 \pm 1.2 \pm 1.9)\%, \tag{28}$$

and using the prediction of Bauer et al. [19]

$$\frac{\mathrm{Br}(B_d \to D^{*-} \ell^+ \nu)}{\mathrm{Br}(B_d \to D^- \ell^+ \nu)} \simeq 2\text{–}3, \tag{29}$$

we get $\mathrm{Br}(B_d \to D \ell X) \simeq 10\%$. The measured value of the average inclusive semileptonic branching ratio for B^0, B^+, B^- is about 12% [20], thus

$$\mathrm{Br}(B_d^0 \to \ell^+ X) \leqslant 12\%. \tag{30}$$

This leaves at most a 2% branching ratio for B_d semileptonic decays not involving D mesons. Among these modes $B_d \to \ell D_s X$ should contribute at best a fraction of $\frac{1}{5}$, since the production of the D_s requires the creation of an additional $s\bar{s}$ pair (see fig. 2), and the ratios of production probabilities are approximately $u\bar{u} : d\bar{d} : s\bar{s} = 2:2:1$. This fraction should get further reduced by the possibility of creating different strange final states. From these we derive the upper bound

$$\mathrm{Br}(B_d \to \ell^+ D_s^- X) \leqslant 0.4\%, \tag{31}$$

but we hope that some experimental information on this branching ratio will become available in the near future. Fig. 2 can be also used as a guideline to estimate the rejection efficiency ε. It suggests that, unlike in the B_s case, most of the D_s's produced in B_d decays are accompanied by at least one K meson. For the sake of a conservative estimate we assume these to be neutral K's, 30% of which can be

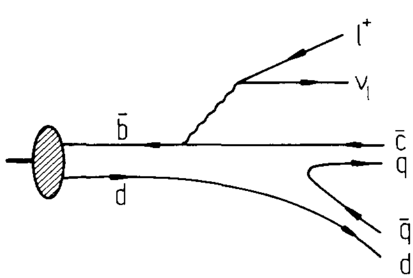

Fig. 2. The Feynman diagram for B_d semileptonic decay into a final state with two mesons.

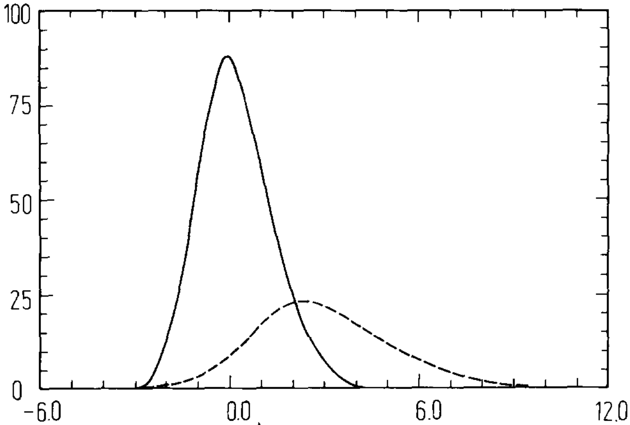

Fig. 3. The missing mass (M^2, see text) distribution for the decays $B_s^0 \to D_s^- \ell^+ \nu$ (solid line) and $B_d^0 \to D_s^- \ell^+ \nu X$ (dashed line). Only phase space is taken into account.

detected and therefore excluded from the sample, i.e. $\varepsilon \simeq 0.7$. Finally, we arrive at:

$$k_{\text{eff}} \geqslant 35 \frac{\hat{s}_e}{\hat{d}_e + \hat{d}_o} . \tag{32}$$

A method to increase k_{eff} even further has been brought to our attention by Nakada [21]. Following a technique used by ARGUS [22], it consists of imposing an appropriate cut on $M^2 \equiv [(m_{B_s} - E_{D_s} - E_\ell)^2 - (\boldsymbol{p}_{D_s} + \boldsymbol{p}_\ell)^2]$, i.e. the square of missing mass. Care must be taken that the lepton and the D_s both originate from the same B meson. In the case of a B_s at rest, M^2 corresponds to the neutrino mass. At the $\Upsilon(5S)$ resonance B_s mesons are produced with small but nonzero momentum. Therefore one expects a distribution in M^2 centered close to zero, but broadened. Calculating M^2 for B_d decays will result in a distribution which is centered at a larger value. This is caused by two reasons. First of all, one uses m_{B_s} instead of m_{B_d} in the formula for M^2. Secondly, the invariant mass of undetected particles cannot be smaller than m_K^2. We calculated the M^2 distribution using the Monte Carlo program JETSET [23], taking into account only phase space. As can be seen from the result, which is shown in fig. 3 (arbitrary normalization), one can eliminate 90% of the B_d contamination while losing only 50% of the B_s signal by cutting on a value of $M^2 = 0$. This increases k_{eff} by a further factor of 5. This agrees well with the results of a Monte Carlo simulation by Nakada [24], where the more realistic transition matrix elements of Bauer, Stech and Wirbel [19] were taken into account for the B decays into final states involving two mesons. We conclude that a value of $k_{\text{eff}} \simeq 45$ is not out of reach. Taking this as an estimate, assuming $\Delta k = 0.5k$,

$\Delta x_d = 0.2$, using Δf_p as in eq. (25), and adding errors in quadrature, we find

$$\Delta R_{s_e} \simeq \sqrt{(2.5\times 10^{-2})^2 + (1.05\Delta\tilde{R})^2}\,. \tag{33}$$

In order to determine R_{s_e} with a precision of at least 10% one therefore has to know $\tilde{R}$ to better than 9%.

One question we still have to address concerns the λ, ρ and k dependence of $\tilde{R}$ (eq. (14)). As we have already mentioned, the parameters λ and ρ are not affected by the specification of the final state. From eq. (14) we find

$$\left|\frac{\partial\tilde{R}}{\partial\lambda}\right|\Delta\lambda \approx \frac{2.1}{k_{\text{eff}}}\Delta\lambda = 0.014, \qquad \text{for } k_{\text{eff}} = 45 \tag{34a}$$

$$\left|\frac{\partial\tilde{R}}{\partial\rho}\right|\Delta\rho \approx \frac{1.4}{k_{\text{eff}}}\Delta\rho = 0.031, \qquad \text{for } k_{\text{eff}} = 45 \tag{34b}$$

$$\left|\frac{\partial\tilde{R}}{\partial k_{\text{eff}}}\right|\Delta k_{\text{eff}} \approx \frac{3.8}{k_{\text{eff}}^2}\Delta k_{\text{eff}} = 0.042, \qquad \text{for } k_{\text{eff}} = 45 \tag{34c}$$

where we have used $\Delta\lambda = 0.3$, $\Delta\rho = \rho = 1$, and $\Delta k = 0.5k$. Combining all the errors, we obtain

$$\Delta R_{s_e} \simeq \sqrt{(6.2\times 10^{-2})^2 + \left(1.05[\Delta\tilde{R}]_{\text{stat}}\right)^2}\,, \tag{35}$$

where

$$(\Delta\tilde{R})_{\text{stat}} \simeq \sqrt{\frac{\tilde{R}(1+\tilde{R})}{N^{+-}}}\,. \tag{36}$$

This calls for 800 $B\bar{B} \to \ell^+\ell^- D_s X$ decays in order to achieve 5% precision in $\tilde{R}$ (i.e. 8% in R_s). In order to estimate the corresponding number of $b\bar{b}$ pairs, we have to take into account the following factors:

(a) 1/0.16 for requiring that the initial $b\bar{b}$ pairs hadronize into one of the $B_s^0\bar{B}_s^0$ states (see table 1),

(b) 2 due to the fact that approximately half of the $B_s^0\bar{B}_s^0$ pairs give rise to opposite sign dileptons,

(c) 2 due to the cut on the missing mass distribution,

(d) 800 for the required statistics,

(e) $(8.4\times 10^{-4})^{-1}$ from the product of branching ratios of interest (we assume that the D_s is detected through its $\phi\pi$ decay mode),

(f) a factor of about 8 for detection efficiency and energy cuts.

This amounts to 2×10^8 $b\bar{b}$ pairs required. Let us give two examples on how this number can constrain the range of x_s in the standard model. First, suppose that the measured value of R_s turns out to be 1.0 ± 0.08. In this case one would derive a lower limit on x_s of 4.8 but no upper bound. On the other hand, if one found a value of $R_s=0.9\pm0.08$, one would get a range $3.0\leqslant x_s\leqslant 9.9$ at the 1 standard deviation level. In our opinion, this method will not be able to yield much more information than indicated above.

2.4. SINGLE-PARTICLE INITIAL STATES

As has been indicated in the previous sections, experiments which do not distinguish between the mixings of the B_d^0–$\bar{B}_d^0$ and the B_s^0–$\bar{B}_s^0$ systems cannot reach the accuracy needed. This is mainly due to the uncertainties in the production probabilities p_d and p_s of the respective mesons. A method sensitive to B_s^0–$\bar{B}_s^0$ mixing only has been proposed by Ali and Barreiro [25]. Their suggestion is to look at the quantity

$$\Delta(\ell KK)=\frac{\sigma(\ell^-K^-K^-)-\sigma(\ell^-K^+K^+)}{\sigma(\ell^-K^-K^-)+\sigma(\ell^-K^+K^+)}, \tag{37}$$

where all three particles belong to the same jet. On the basis of statistical errors only, a relatively small number of 5×10^5 $b\bar{b}$ pairs is necessary in order to obtain the required 10% accuracy in R_s. However, a reasonable estimate of various uncertainties (such as the dependence on p_s and needed branching ratios, K–π misidentification, and choice of fragmentation model), as already indicated in ref. [25], leads to the conclusion that $\Delta(\ell KK)$ is at best sensitive to $x_s\leqslant 2$. Therefore this still could be an excellent method, but in the case of small x_s.

As a further example of this type of measurement, we consider the production of $b\bar{b}$ quark pairs at energies high above the $\Upsilon(5S)$ mass, at a Z^0 factory, for example. For the reasons discussed in sect. 2.1, we examine only single-particle initial states. In order to facilitate the identification of the B's, we consider initial states where the B_s meson is produced along with a charged B (either $B_u^\pm$ or $B_c^\pm$). We then require that the charged B be fully reconstructed, and that the B_s meson be identified through its semi-leptonic decay mode $B_s\to\ell D_sX$. r_s (eq. (2)) is then obtained by taking the ratio of the number of events in which the charged B and the lepton have the same sign and the number of events in which they have opposite signs.

However, the possibility of B_d and charged B decays to final states which include a lepton and a D_s must also be taken into account. For both B_d and B_u mesons, these decays are suppressed relative to the B_s decays. Although nothing is known about $B_c^\pm$'s, the decay $B_c\to\ell D_sX$ also requires the creation of a quark pair from the vacuum. We will therefore assume this suppression ε to be the same for all cases. As shown previously, $\varepsilon\simeq0.04$. There is also the possibility of error in determining the charge of the $B^{\pm}_{u,c}$. We will denote this error as α. Finally, a lepton and a D_s can be produced from other sources and these backgrounds must also be taken into account. The size of this background depends on the experiment; we will parametrize it by a quantity β defined as $[N(\ell D_s)_{tot} - N(\ell D_s)_{from\ B_s}]/N(\ell D_s)_{from\ B_s}$. Assuming that the background contribution to the same sign events is equal to that for the opposite sign events, we have

$$r_{exp} = \left[(1-\alpha)\frac{p_s r_s}{1+r_s} + \alpha\frac{p_s}{1+r_s} + \varepsilon(1-\alpha)\frac{p_d r_d}{1+r_d} + \varepsilon\alpha\frac{p_d}{1+r_d} + \varepsilon\alpha p_{ch} + \beta\right]$$
$$\times\left[(1-\alpha)\frac{p_s}{1+r_s} + \alpha\frac{p_s r_s}{1+r_s} + \varepsilon(1-\alpha)\frac{p_d}{1+r_d} + \varepsilon\alpha\frac{p_d r_d}{1+r_d} + \varepsilon(1-\alpha)p_{ch} + \beta\right]^{-1} \tag{38}$$

where again p_s is the probability that a b quark hadronizes into a B_s meson, and p_d and p_{ch} are defined similarly for the B_d's and charged B's, respectively.

We now estimate the effects of the various uncertainties on the error Δr_s. For simplicity, we neglect α (which is expected to be small in any case). Then r_s can be expressed as a function of r_{exp} and the parameters κ, κ', and γ, which are defined as

$$\kappa = \varepsilon\frac{p_d}{p_s}, \qquad \kappa' = \varepsilon\frac{p_{ch}}{p_s}, \qquad \gamma = \frac{\beta}{p_s}. \tag{39}$$

Assuming that $p_u : p_d : p_s \simeq 2:2:1$, and ignoring the effects of $c\bar{c}$ quark pairs, yields $\kappa \simeq \kappa' \simeq 0.08$. Using these values for κ and κ', and taking $r_s \simeq 1$, one finds

$$\frac{\partial r_s}{\partial r_{exp}} = \frac{(2\gamma + 1.3)^2}{2\gamma + 1.16}. \tag{40}$$

Requiring that this derivative be less than 2 (which, together with our 10% accuracy requirement for r_s, corresponds to $\Delta r_{exp} < 5\%$) constrains γ to be $0 < \gamma < 0.27$, and we assume that the background can be reduced to this value ($\beta < 0.05$). This in turn constrains the other contributions to Δr_s to be in the ranges

$$0 < |\partial r_s/\partial\gamma|\gamma < 0.02, \tag{41a}$$

$$1.11\Delta\kappa < |\partial r_s/\partial\kappa|\,\Delta\kappa < 1.18\Delta\kappa, \tag{41b}$$

$$1.78\Delta\kappa' < |\partial r_s/\partial\kappa'|\,\Delta\kappa' < 1.85\Delta\kappa', \tag{41c}$$

where we have taken $\Delta\gamma \simeq \gamma$. To estimate the number of $b\bar{b}$ pairs required, we

assume that $\Delta r_s = 0.08$ and $\gamma = 0.27$. For values of the errors $\Delta\kappa/\kappa$ and $\Delta\kappa'/\kappa'$ equal to 25% (0%), this calls for $\Delta r_{exp}/r_{exp} < 2.5\%$ (4%). With the following factors:
(a) 25/2 for requiring that the initial $b\bar{b}$ pair hadronize into $B_s^0B^-$ or $\bar{B}_s^0B^+$,
(b) 10 for the efficiency of reconstructing the charged B,
(c) 2500 ($\Delta r_{exp}/r_{exp} = 4\%$) – 6400 ($\Delta r_{exp}/r_{exp} = 2.5\%$) for the required statistics,
(d) $(6 \times 10^{-3})^{-1}$ from the product of branching ratios of interest,
(e) 5 for the efficiency of detecting the ℓD_s final state,
we find that 3–7×10^8 $b\bar{b}$ quark pairs are required. Of course, should the background be larger ($\beta > 0.05$), even more $b\bar{b}$ pairs are needed.

3. Time dependent methods

Due to mixing, the interaction and mass eigenstates of B_s mesons do not coincide. This can be observed as oscillations (as a function of proper time) of the number of decays to final states accessible only for the weak eigenstate B_s^0 but not for $\bar{B}_s^0$ (or vice versa). The measurement of x_s then consists of observing the oscillations and determining their frequency. Such a measurement requires a quite different experimental situation than that utilized in the previous section. Due to the short lifetime of B mesons, a large boost is necessary so that the b and $\bar{b}$ quarks are produced with large momenta in the laboratory system. There are two possibilities for such experiments – either at energies high above the threshold for $B_s^0\bar{B}_s^0$ production [26], or at an asymmetric e^+e^- collider at a centre of mass energy near the $\Upsilon(5S)$ mass [27]. We now discuss these cases in turn (ignoring *CP* violating effects and lifetime differences).

3.1. OSCILLATIONS HIGH ABOVE THE $B_s^0\bar{B}_s^0$ THRESHOLD

Experiments examining the time-dependence of B_s oscillations high above threshold could, in principle, be carried out at Z^0 factories, high energy hadron colliders, fixed target machines, or ep colliders. Regardless of which machine is used for this experiment, the program for measuring the time-dependence of the oscillations is as follows:
(i) Look for the decay of a B_s meson.
(ii) Measure the time t at which it decayed, and identify whether it was a B_s^0 or a $\bar{B}_s^0$ at this time.
(iii) Look on the other side for the decay of another B and determine whether the decaying B meson contained a b or a $\bar{b}$ quark. (We will generically refer to a meson containing a $\bar{b}$ quark as a B; a $\bar{B}$ meson contains a b quark.)
(iv) Plot $N(B_s^0\bar{B} + \bar{B}_s^0B)$ vs. t and $N(B_s^0B + \bar{B}_s^0\bar{B})$ vs. t. x_s can then be obtained from the period of oscillation of these curves.

There are three types of initial states which contain a B_s meson. First of all, B_s's can be produced along with charged B's, i.e. $B_s^0B^-$ and $\bar{B}_s^0B^+$. Since the charged B's cannot oscillate, the respective distributions, as a function of the B_s proper time t, are given by

$$\left.\begin{array}{l} N\left(B^- B_s^0 \to B^- B_s^0;\, t\right) \\ N\left(B^- B_s^0 \to B^- \overline{B}_s^0;\, t\right) \end{array}\right\} \sim \tfrac{1}{2}\exp\left(-\frac{t}{\tau}\right)\left[1 \pm \cos\left(x_s \frac{t}{\tau}\right)\right], \tag{42}$$

where τ is the lifetime of the B_s meson. Similar equations are obtained for the case in which the initial state is $B^+\overline{B}_s^0$. Secondly, $B_s^0\overline{B}_d^0$ and $\overline{B}_s^0 B_d^0$ pairs can be produced. Here, the B_d mesons can also oscillate, but the oscillations of the B_d and B_s are independent. In this case we must integrate over the decay time of the B_d, since this time is not measured. This gives

$$\left.\begin{array}{l} N\left(B_d^0\overline{B}_s^0 \to B_d^0\overline{B}_s^0;\, t\right) + N\left(B_d^0\overline{B}_s^0 \to \overline{B}_d^0 B_s^0;\, t\right) \\ N\left(B_d^0\overline{B}_s^0 \to \overline{B}_d^0\overline{B}_s^0;\, t\right) + N\left(B_d^0\overline{B}_s^0 \to B_d^0 B_s^0;\, t\right) \end{array}\right\} \sim \tfrac{1}{2}\exp\left(-\frac{t}{\tau}\right)\left[1 \pm \frac{1}{1+x_d^2}\cos\left(x_s \frac{t}{\tau}\right)\right]. \tag{43}$$

Similar equations result when the initial state is $\overline{B}_d^0 B_s^0$. Finally, $B_s^0\overline{B}_s^0$ pairs can also be produced. These are produced along with other particles, and therefore constitute an incoherent state of angular momentum. Because of this, this situation is completely analogous to the case in which the initial state is $B_d^0\overline{B}_s^0$ or $\overline{B}_d^0 B_s^0$, yielding

$$\left.\begin{array}{c} N\left(B_s^0\overline{B}_s^0 \to B_s^0\overline{B}_s^0;\, t\right) \\ N\left(B_s^0\overline{B}_s^0 \to \overline{B}_s^0\overline{B}_s^0;\, t\right) + N\left(B_s^0\overline{B}_s^0 \to B_s^0 B_s^0;\, t\right) \end{array}\right\} \sim \tfrac{1}{2}\exp\left(-\frac{t}{\tau}\right)\left[1 \pm \frac{1}{1+x_s^2}\cos\left(x_s \frac{t}{\tau}\right)\right]. \tag{44}$$

Combining eqs. (42), (43) and (44) we obtain

$$N\left(B_s^0\overline{B} + \overline{B}_s^0 B;\, t\right) \sim \tfrac{1}{2}\exp(-t/\tau)\left[1 + \left\{\left(\frac{1}{1+x_s^2} + R_1\frac{1}{1+x_d^2} + R_2\right)\Big/(1+R_1+R_2)\right\}\cos\left(x_s\frac{t}{\tau}\right)\right], \tag{45a}$$

$$N\left(B_s^0 B + \overline{B}_s^0\overline{B};\, t\right) \sim \tfrac{1}{2}\exp(-t/\tau)\left[1 - \left\{\left(\frac{1}{1+x_s^2} + R_1\frac{1}{1+x_d^2} + R_2\right)\Big/(1+R_1+R_2)\right\}\cos\left(x_s\frac{t}{\tau}\right)\right]. \tag{45b}$$

where

$$R_1 = \frac{N(\bar{B}_d^0 B_s^0) + N(B_d^0 \bar{B}_s^0)}{N(B_s^0 \bar{B}_s^0)}, \qquad R_2 = \frac{N(B^- B_s^0) + N(B^+ \bar{B}_s^0)}{N(B_s^0 \bar{B}_s^0)}. \tag{46}$$

Using the continuum production ratios $u\bar{u} : d\bar{d} : s\bar{s} = 2:2:1$, we estimate $R_1 \simeq R_2 \simeq 2$.

In the following we discuss the experimental errors which have to be taken into account in obtaining these distributions. First of all, in order to determine whether it was a B_s^0 or a $\bar{B}_s^0$ which decayed, one must search for final states to which only B_s^0 or $\bar{B}_s^0$ can decay. One example of such a decay is $B_s^0 \to D_s^- + (n\pi)^+$ (or $\bar{B}_s^0 \to D_s^+ + (n\pi)^-$). In this case the charge of the D_s tags the decaying particle. Secondly, the simplest way to see whether the other decaying B contained a b or a $\bar{b}$ quark is to look at semi-leptonic decays. In this case, the charge of the $\ell^\pm$ can then be used as a tag. For both the $D_s^\pm$ and the $\ell^\pm$ there is a finite probability for mistagging the charge of the meson. The effect of this error is to combine the distributions in eqs. (45a) and (45b), thereby reducing the signal. In the following, we will assume this mistagging error to be 15%. Finally, the proper time is not obtained directly – it must be extracted from the distance of flight and the energy measurements. The average distance travelled by B_s in the course of its lifetime is given by:

$$l_\tau = \frac{cE\tau}{m_{B_s}} \approx 1.9 \left[\frac{E}{30\ \text{GeV}}\right] \left[\frac{\tau}{1.1 \times 10^{-12}\ \text{s}}\right] \text{mm}. \tag{47}$$

For energetic B_s mesons, the next generation of vertex detectors will be able to determine this length with reasonable precision. For such detectors, we will take Δl to be 25 μm (this is only slightly more optimistic than the 30 μm expected for the ARGUS upgrade [28], but more conservative than the 10 μm used in ref. [27]). For the relative error in the proper time measurement one gets:

$$\frac{\Delta t}{t} \sim \frac{\Delta t}{\tau} \approx \sqrt{\left(\frac{m_B \Delta l}{cE\tau}\right)^2 + \left(\frac{\Delta E}{E\beta^2}\right)^2}\,. \tag{48}$$

Taking $E = 15$ GeV as an estimate, a 10% relative error in the energy determination leads to $\Delta t/\tau \simeq O$ (10%). Nonvanishing Δt limits the range of x_s to which this kind of technique is sensitive since it leads to a smearing of the actually observed distributions.

To simulate the effect of the $\Delta t/\tau$ error, we convolute the function in eq. (45a) with a gaussian error factor* (the analysis is similar for eq. (45b)). In fig. 4 we show

* This constitutes only a rough approximation of the real experimental situation; a detailed Monte Carlo analysis could model it more accurately. However, we think that our method incorporates the main features and therefore our conclusions should not be changed dramatically.

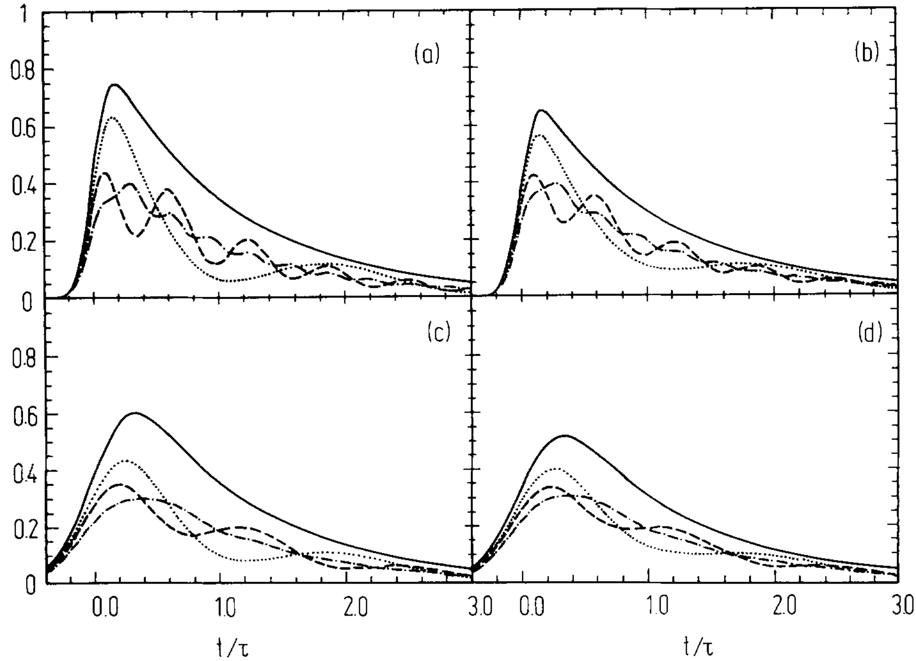

Fig. 4. The distribution $N(B_s^0\bar{B} + \bar{B}_s^0 B; t)$ (eq. (45a)), folded with a gaussian factor as a function of the proper time t/τ: (a) without charge misidentification, and with $\Delta t/\tau = 0.1$, for $x_s = 0$ (solid), 3 (dotted), 10 (dashed), and 20 (dot-dashed); (b) as in (a), but now with a 15% probability for charge misidentification; (c) without charge misidentification, but with $\Delta t/\tau = 0.25$, for $x_s = 0$ (solid), 3 (dotted), 5 (dashed), and 10 (dot-dashed); (d) as in (c), but now with a 15% probability for charge misidentification.

how the gaussian smearing affects the shape of the distribution with and without mistagging (figs. 4b and 4a, respectively) for $\Delta t/\tau = 0.10$ and $x_s = 0$, 3, 10 and 20. (In these figures and those following, we take $R_1 = R_2 = 2$.) Because of the nonzero $\Delta t/\tau$ error, the curves develop a tail for $t/\tau < 0$. In order to compare these figures with experimental results, one has to multiply the distributions of fig. 4 by the total number of experimental events. (This same normalization is used in figs. 5 and 7.) One sees that with such an accuracy the range $3 \leqslant x_s \leqslant 15$ is accessible. In fact, even smaller values of x_s can be obtained using this method. However, there is a lower bound of about $x_s = 1$ which originates from the fact that for small mixing the distribution is very close to the purely exponential one, even in the case of vanishing proper time and mistagging errors. For less accurate proper time measurements this range is reduced considerably. For example, in figs. 4c (no mistagging) and 4d (mistagging included), we plot the curves for $\Delta t/\tau = 0.25$ and $x_s = 3, 5, 10$. For this proper time error, only $3 \leqslant x_s \leqslant 8$ appears to be accessible. However, with reasonable precision on $\Delta t/\tau$, this method is sensitive to quite large values of x_s. In order to visualize the importance of precise proper time measurements, in fig. 5 we plot

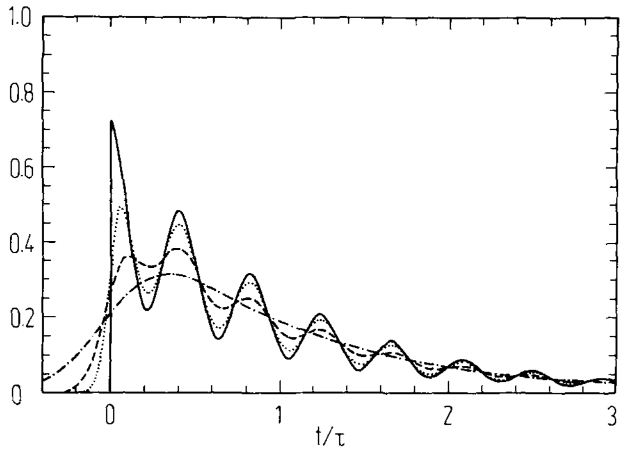

Fig. 5. The distribution $N(B_s^0\bar{B}+\bar{B}_s^0B;\,t)$ (eq. (45a)), for a fixed value of $x_s = 15$, convoluted with the error factor corresponding to $\Delta t/\tau = 0$ (solid), 0.05 (dotted), 0.1 (dashed), and 0.25 (dot-dashed).

the distributions (including the mistagging error) for a fixed value of $x_s = 15$ and several values of $\Delta t/\tau$ (0, 0.05, 0.1, 0.25).

We note an interesting feature of the distributions under consideration. The value of the ratio $N(B_s^0B+\bar{B}_s^0\bar{B};\,t)/N(B_s^0\bar{B}+\bar{B}_s^0B;\,t)$ at any given fixed time t is not a constant – it depends on the values of $\Delta t/\tau$ and x_s. Using our procedure for taking the experimental errors into account, this is illustrated in fig. 6, for $t/\tau = 2\pi/x_s$ (i.e. for the value at which the distribution in the numerator develops a minimum for $\Delta t = 0$). Although a Monte Carlo simulation is needed in order to determine the actual size of the effect, it may provide additional information on x_s.

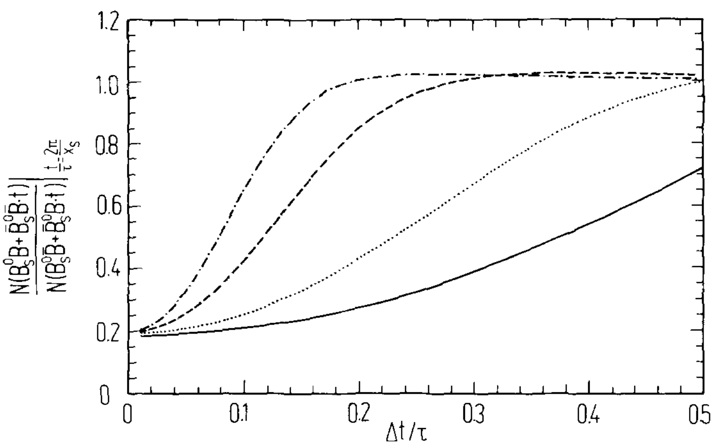

Fig. 6. The ratio $N(B_s^0B+\bar{B}_s^0\bar{B};\,t)/N(B_s^0\bar{B}+\bar{B}_s^0B;\,t)$ at $t/\tau = 2\pi/x_s$ as a function of the error $\Delta t/\tau$ for $x_s = 3$ (solid), 5 (dotted), 10 (dashed), and 15 (dot-dashed).

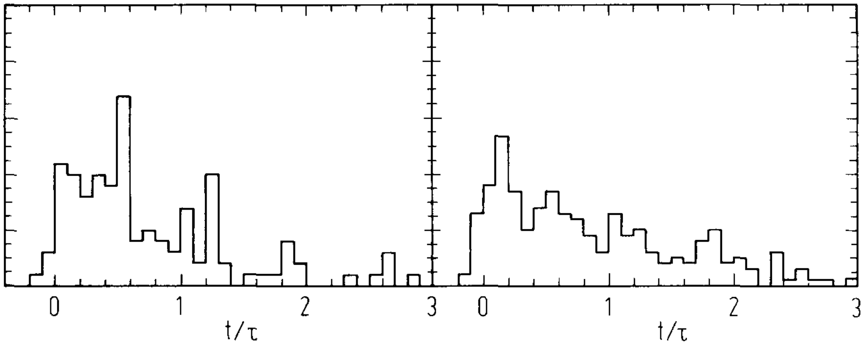

Fig. 7. Simulation of the actual experimental data (see text) for the distribution $N(B_s^0\bar{B} + \bar{B}_s^0 B; t)$ with $x_s = 10$ and (a) 250, (b) 500 reconstructed B_s^0 or $\bar{B}_s^0$ mesons.

In order to estimate the number of events needed to see the oscillations, we simulated the real experimental situation by transforming our continuous distributions into histograms as follows. For $x_s = 10$, and including both a mistagging error of 15% and an error $\Delta t/\tau = 0.1$, the distribution of eq. (45a) is split into bins of size equal to the error in the proper time. The number of events in each bin is then interpreted as a mean of the Poisson distribution, and a random number is generated accordingly. This number is then taken to be the actual height of the bin. We present the histograms for a total of 250 events (fig. 7a) and 500 events (fig. 7b). Although it would be difficult to see an oscillation signal with 250 events, it should be possible with 500 events. However, we note that, for $\Delta t/\tau = 0.25$ (and corresponding bin size), the oscillations become essentially invisible.

We now estimate the total number of $b\bar{b}$ pairs required. Since we are looking for oscillations in $N(B_s^0\bar{B} + \bar{B}_s^0 B; t)$ or $N(B_s^0 B + \bar{B}_s^0\bar{B}; t)$, the final state to which the B_s decays must be chosen carefully. A total energy measurement is required, so that semileptonic decays are of no use here. For the case of hadronic decay modes, these should have relatively large branching ratios and reasonable detection efficiencies. In general, the oscillation signal will lie on top of an essentially exponential background coming from B_d^0 and $\bar{B}_d^0$ decays. Since the ratio of B_s to B_d mesons in the initial state is expected to be of order 1 : 2, it is useful to consider modes that distinguish B_s from B_d. Also, as noted earlier, the final state must distinguish B_s^0 from $\bar{B}_s^0$. As an indicative example we consider the following decay chain:

$$
\begin{aligned}
b\bar{b} \to\ & B^+\bar{B}_s^0 X \\
& \hookrightarrow D_s^{+*} + (n\pi)^- \\
& \qquad \hookrightarrow D_s^+\gamma\ (150\ \text{MeV}) \\
& \qquad\qquad \hookrightarrow \phi\pi \\
& \qquad\qquad\quad \hookrightarrow K^+K^- .
\end{aligned}
\tag{49}
$$

The branching ratio for $\bar{B}_s^0 \to D_s^{+*} + (n\pi)^-$ can be estimated by comparison with $Br(\bar{B}_d \to D^{+*} + (n\pi)^-)$, where the sum over various numbers of charged π's (needed for good vertex identification and energy reconstruction) gives about 5% [18]. The other factors which enter our estimate are

(a) a factor of about 5 for requiring that the initial $b\bar{b}$ pairs hadronize into at least one B_s^0 or $\bar{B}_s^0$,

(b) 10 due to the tagging on the charged lepton (i.e. it must be certain that this lepton comes from the decay of a B meson),

(c) 10 or more originating from detection efficiency, energy cuts, K–π misidentification, background subtraction, etc.,

(d) 500 for the required statistics,

(e) $(1.5 \times 10^{-3})^{-1}$ from the product of branching ratios of interest.

This amounts to at least 3×10^8 $b\bar{b}$ pairs needed. One way to reduce this number would be to reduce the uncertainties in items (b) and (c). Another possibility might be to sum over various decay modes of the D_s to reduce the effect of the branching ratios (item (e)).

3.2. OSCILLATIONS NEAR THE $B_s^0\bar{B}_s^0$ THRESHOLD

The experimental situation is quite different at energies near the $B_s^0\bar{B}_s^0$ threshold, i.e. around the $\Upsilon(5S)$. First of all, because of energy considerations, B_s mesons can only be produced in the initial state $B_s^0\bar{B}_s^0$, or from the decays of the excited states $B_s^*\bar{B}_s$, $B_s\bar{B}_s^*$, or $B_s^*\bar{B}_s^*$. In any of these cases, the $B_s^0\bar{B}_s^0$ pair is produced in a definite state of angular momentum. For this two particle initial state, the expressions for the oscillations depend on the angular momentum of the $B_s^0\bar{B}_s^0$ system:

$$N\left(B_s^0\bar{B}_s^0 \to B_s^0\bar{B}_s^0;\, t_1, t_2\right) \sim \exp\left(-\frac{t_1+t_2}{\tau}\right)\begin{cases} \cos^2\left(\dfrac{x_s}{2}\dfrac{t_1+t_2}{\tau}\right), & \text{for } L \text{ even;} \\ \cos^2\left(\dfrac{x_s}{2}\dfrac{t_1-t_2}{\tau}\right), & \text{for } L \text{ odd.} \end{cases} \tag{50a}$$

$$N\left(B_s^0\bar{B}_s^0 \to B_s^0B_s^0;\, t_1, t_2\right) + N\left(B_s^0\bar{B}_s^0 \to \bar{B}_s^0\bar{B}_s^0;\, t_1, t_2\right)$$

$$\sim \exp\left(-\frac{t_1+t_2}{\tau}\right)\begin{cases} \sin^2\left(\dfrac{x_s}{2}\dfrac{t_1+t_2}{\tau}\right), & \text{for } L \text{ even;} \\ \sin^2\left(\dfrac{x_s}{2}\dfrac{t_1-t_2}{\tau}\right), & \text{for } L \text{ odd.} \end{cases} \tag{50b}$$

In eq. (50), t_1 and t_2 are the proper times of the initial B_s^0 and $\bar{B}_s^0$, respectively. Another feature of the $\Upsilon(5S)$ is that the $B_s\bar{B}_s$ pair is produced almost at rest in the center of mass. However, as noted earlier, in order to measure the decay times, it is necessary to produce the $B_s^0\bar{B}_s^0$ system with a definite boost in the lab system. This can be achieved with an asymmetric e^+e^- collider [27].

With such a machine, the method for obtaining x_s from a time-dependent measurement is somewhat different from that in sect. 3.1. Although the energy of the B's is known approximately, the beam interaction point is not, so that t_1 and t_2 cannot be individually determined. However, the B_s^0–$\bar{B}_s^0$ proper time difference is an accessible quantity. Integrating eq. (50) with respect to $t_1 + t_2$, while keeping $t_1 - t_2$ fixed, results in the following distributions in $|t_1 - t_2|$:

$$N\left(B_s^0\bar{B}_s^0 \to B_s^0\bar{B}_s^0;\, |t_1 - t_2|\right)$$
$$\sim \tfrac{1}{2}\exp\left(-\frac{|t_1 - t_2|}{\tau}\right)\begin{cases} \dfrac{1}{1+x_s^2}\left\{2\cos^2\left(\dfrac{x_s}{2}\dfrac{t_1 - t_2}{\tau}\right) + x_s^2 - x_s\sin\left(x_s\dfrac{|t_1 - t_2|}{\tau}\right)\right\}, & L \text{ even}, \\ 2\cos^2\left(\dfrac{x_s}{2}\dfrac{t_1 - t_2}{\tau}\right), & L \text{ odd}. \end{cases} \tag{51a}$$

$$N\left(B_s^0\bar{B}_s^0 \to B_s^0 B_s^0;\, |t_1 - t_2|\right) + N\left(B_s^0\bar{B}_s^0 \to \bar{B}_s^0\bar{B}_s^0;\, |t_1 - t_2|\right)$$
$$\sim \tfrac{1}{2}\exp\left(-\frac{|t_1 - t_2|}{\tau}\right)\begin{cases} \dfrac{1}{1+x_s^2}\left\{2\sin^2\left(\dfrac{x_s}{2}\dfrac{t_1 - t_2}{\tau}\right) + x_s^2 + x_s\sin\left(x_s\dfrac{|t_1 - t_2|}{\tau}\right)\right\}, & L \text{ even}, \\ 2\sin^2\left(\dfrac{x_s}{2}\dfrac{t_1 - t_2}{\tau}\right), & L \text{ odd}. \end{cases} \tag{51b}$$

As suggested by Feldman [29], these two different classes of distributions can be observed as oscillations in the number of opposite and same sign dileptons. These signals will be on top of an almost exponential background coming from B_d and $B^\pm$ decays. However, in principle, one would expect a drastic reduction in the number of b quarks required to obtain x_s, since one can look at inclusive semileptonic decays of B_s mesons, which have large branching ratios and for which detection efficiencies are good.

Of course, these distributions are affected by experimental errors. First of all, there is an important systematic error [14] due to the fact that $B\bar{B}$ pairs are not produced at rest in the centre of mass system (i.e. the Doppler effect). If they were at rest in the CM system, then, by knowing the relative velocity β of the laboratory and CM systems, it would be possible to obtain the proper time difference $t_1 - t_2$

quite accurately. However, the distance between the decay vertices of the two B mesons in the lab system is approximately given by*

$$d = c\gamma\beta(t_1 - t_2) + c\gamma\beta_{\rm cm}\cos(\theta_{\rm cm})(t_1 + t_2) + {\rm O}(\beta_{\rm cm}^2), \tag{52}$$

where $\beta_{\rm cm}$ is the velocity of the B mesons in the centre of mass system, and $\theta_{\rm cm}$ denotes the polar angle with respect to the beam pipe at which this meson is emitted in the CM. Taking $\langle t_1 + t_2 \rangle \simeq 2\tau$ and $\langle |\cos\theta_{\rm cm}| \rangle = 2/\pi$, this leads to a systematic error in $(t_1 - t_2)$ as extracted from d:

$$\left[\frac{\Delta(t_1 - t_2)}{\tau}\right]_{\rm syst} \simeq \frac{4}{\pi}\frac{\beta_{\rm cm}}{\beta} \simeq 1.8\beta_{\rm cm}. \tag{53}$$

In the last step we have assumed a 12.5 GeV on 2.3 GeV collider configuration as proposed in ref. [27]. This Doppler effect affects different modes in different ways. For example, with the centre of mass energy just above the threshold for $B_s^*\bar{B}_s^*$ production, one finds that $B_s\bar{B}_s$ pairs coming from the decays of $B_s^*\bar{B}_s^*$ have, on average, $\beta_{\rm cm} = 0.01$, while $B_s\bar{B}_s$ pairs produced directly have $\beta_{\rm cm} = 0.14$. For $B\bar{B}$ pairs originating from all the various angular momentum states, we have

$$\begin{array}{lcccccc} & B_s^*\bar{B}_s^*, & B_s\bar{B}_s^* + B_s^*\bar{B}_s, & B_s\bar{B}_s, & B_d^*\bar{B}_d^*, & B_d\bar{B}_d^* + B_d^*\bar{B}_d, & B_d\bar{B}_d \\ \beta_{\rm cm}: & 0.01, & 0.10, & 0.14, & 0.20, & 0.22, & 0.24, \end{array} \tag{54}$$

For the even-L configurations, we have taken the average value of $\beta_{\rm cm}$.

Since the beam energy is expected to be well controlled, the main source of statistical error in $\Delta(t_1 - t_2)/\tau$ is the finite vertex resolution. Assuming this resolution to be 25 μm, one gets

$$\left[\frac{\Delta(t_1 - t_2)}{\tau}\right]_{\rm res} \simeq \frac{25\ \mu{\rm m}\cdot\sqrt{2}}{c\gamma\beta\tau} \simeq 0.1, \tag{55}$$

with the assumed asymmetric collider configuration ($\beta\gamma = 1$). An increase in the asymmetry of the beam energies leads to larger values of $\gamma\beta$ and therefore decreases the systematic uncertainty slightly. However, the statistical error is more complicated – an increase in $\gamma\beta$ in eq. (55) will also result in an increased error in d, caused by the higher collimation of the B decay products. Therefore an optimal choice of the collider configuration might exist which would minimize $[\Delta(t_1 - t_2)/\tau]_{\rm res}$. In the subsequent discussion we assume this minimal value to be given by eq. (55). We will, however, also consider larger values of the statistical

* This assumes that the B's are produced back to back in the CM system. In fact, because of B* and $B\bar{B}\pi$ production, this is not the case. However, a more accurate estimate of this systematic error would require a detailed Monte Carlo simulation.

error. This error sets the upper limit for the value of x_s accessible experimentally. We also note that, because of the systematic error, there is a minimum value of β required to measure x_s, i.e. there is a minimum necessary asymmetry in the beam energies.

Finally, there are two more factors which must be taken into account. First, there is the possibility of charge misidentification. We will assume this error to be equal to 5%, but it turns out that this does not affect the shape of the distributions significantly. A more serious difficulty is due to the background. First, there is a purely exponential component, due to charged B decays. This contributes predominantly to the opposite sign dilepton signal, but due to charge misidentification it also affects the same sign dilepton distribution. Secondly, semileptonic decays of $B_d^0\bar{B}_d^0$ pairs also contribute. Since the $B_d^0\bar{B}_d^0$ production rate is larger than that for $B_s^0\bar{B}_s^0$ pairs, this will constitute a large background which, however, carries a different oscillation frequency. (Since x_d is much less than x_s, the background due to B_d decays will be almost exponential.) Moreover, for both the B_s and B_d components one does not experimentally distinguish between the two different angular momentum eigenstates. Therefore their contributions must be combined with some appropriate weights. Finally, $B\bar{B}$ pairs can be produced in association with charged or neutral π's. As discussed in sect. 2, this contributes to a variety of modes, for example, $B_d^0\bar{B}_d^0\pi^0$, $B^+B^-\pi^0$, $B^+\pi^-\bar{B}_d^0$, etc. The π^0 modes effectively increase the contributions of both B^+B^- pairs and $B_d^0\bar{B}_d^0$ pairs (both even and odd angular momentum). On the other hand, for the contributions with charged π's, one has to take into account a new kind of distribution:

$$N\left(B^+\bar{B}_d^0 \to B^+\bar{B}_d^0;\, t_1, t_2\right) \sim \exp\left(-\frac{t_1+t_2}{\tau}\right)\cos^2\left(\frac{x_d}{2}\frac{t_1}{\tau}\right),$$

$$N\left(B^+\bar{B}_d^0 \to B^+B_d^0;\, t_1, t_2\right) \sim \exp\left(-\frac{t_1+t_2}{\tau}\right)\sin^2\left(\frac{x_d}{2}\frac{t_1}{\tau}\right), \qquad (56)$$

which, after integration over $t_1 + t_2$ and symmetrization with respect to the sign of $t_1 - t_2$, leads to the following expressions:

$$N\left(B^+\bar{B}_d^0 \to B^+\bar{B}_d^0;\, |t_1-t_2|\right) \sim \frac{1}{4+x_d^2}\exp\left(-\frac{|t_1-t_2|}{\tau}\right)\left\{3+\frac{x_d^2}{2}+\cos\left(x_d\frac{|t_1-t_2|}{\tau}\right)-\frac{x_d}{2}\sin\left(x_d\frac{|t_1-t_2|}{\tau}\right)\right\} \qquad (57a)$$

$$N\left(B^+\bar{B}_d^0 \to B^+B_d^0;\, |t_1-t_2|\right) \sim \frac{1}{4+x_d^2}\exp\left(-\frac{|t_1-t_2|}{\tau}\right)\left\{1+\frac{x_d^2}{2}-\cos\left(x_d\frac{|t_1-t_2|}{\tau}\right)+\frac{x_d}{2}\sin\left(x_d\frac{|t_1-t_2|}{\tau}\right)\right\} \qquad (57b)$$

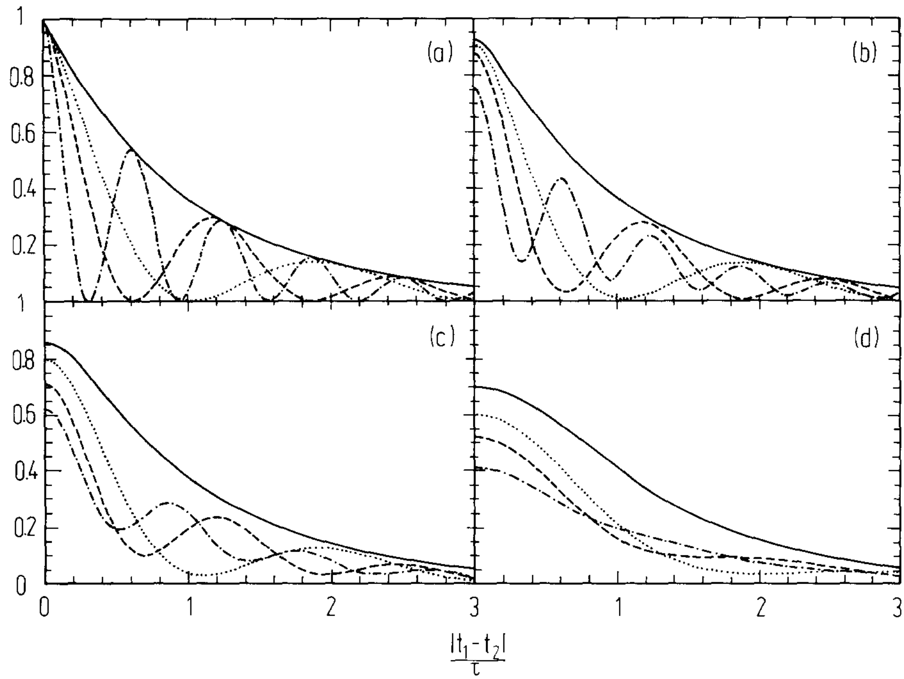

Fig. 8. The distribution $N(B_s^0\bar{B}_s^0 \to B_s^0\bar{B}_s^0; |t_1 - t_2|)$ for L odd (eq. (51a)), as a function of the proper time difference $|t_1 - t_2|/\tau$: (a) for $x_s = 0$ (solid), 3 (dotted), 5 (dashed), and 10 (dot-dashed); (b) as in (a), but now folded with the error factor corresponding to $[\Delta(t_1 - t_2)/\tau]_{res} = 0.1$; (c) as in (b), but now with $[\Delta(t_1 - t_2)/\tau]_{res} = 0.2$; (d) for $x_s = 0$ (solid), 2 (dotted), 3 (dashed), and 5 (dot-dashed), but folded with an error factor corresponding to $[\Delta(t_1 - t_2)/\tau]_{res} = 0.5$.

Similar equations are obtained when the initial state is $B^- B_d^0 \pi^+$. The process of the type (57a) contributes to the opposite sign dilepton signal, whereas the process of type (57b) affects the same sign dilepton rate. For these distributions, the Doppler effect leads to a systematic uncertainty as given in eq. (53) with an average $\beta_{cm} = 0.16$.

We first consider the distributions with opposite sign dileptons only. In fig. 8a we plot the function in eq. (51a), L odd, for four values of x_s (0, 3, 5, 10). In figs. 8b and 8c, we smear this function using a gaussian error factor as in the previous section, for different values of the statistical error, $[\Delta(t_1 - t_2)/\tau]_{res} = (0.1, 0.2)$, while in fig. 8d we use $[\Delta(t_1 - t_2)/\tau]_{res} = 0.5$ and $x_s = (0, 2, 3, 5)$. Neither the systematic error, mistagging error, nor background is taken into account here. Already it can be seen that a statistical error of 0.5 essentially washes out the signal. Analogous curves for L even are given in fig. 9. In both figures the curves are normalized to the number of $B\bar{B}$ pairs initially present with a given angular momentum. One clearly observes that in the case of L even, the amplitude of the oscillation is very small and therefore difficult to detect. This shows that the centre

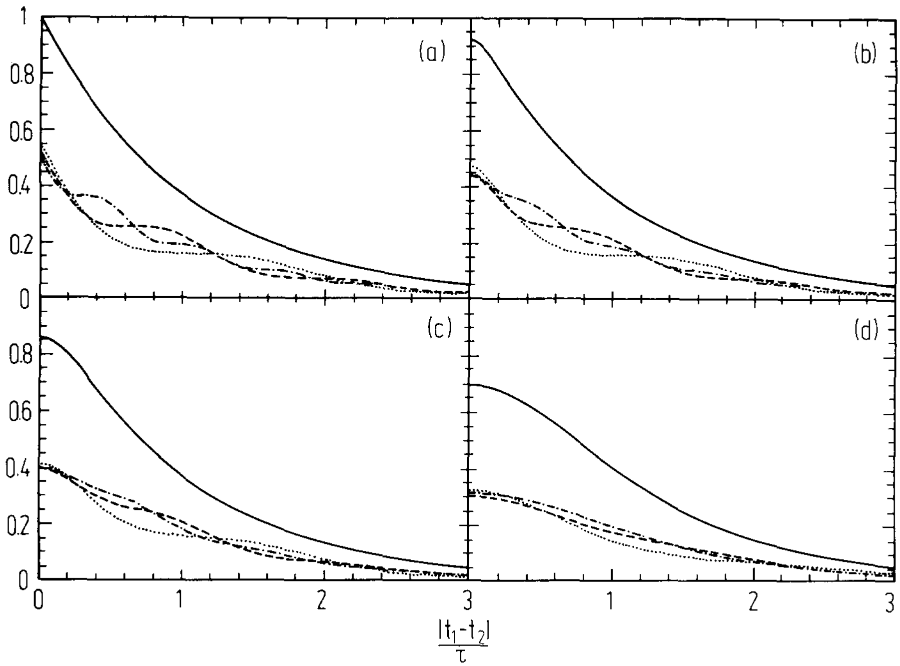

Fig. 9. As in figs. 8(a–d) but for L even.

of mass energy must be adjusted to a value for which the odd-L B_s states predominate. In principle this value could be below the $B_s\bar{B}_s^*$ threshold, which might be preferable in view of the systematic uncertainty caused by the Doppler effect. However, this energy corresponds to the dip in the cross section, as can be seen in fig. 1. Therefore the Υ(5S) would be better suited, if its mass were greater than $2m_{B_s^*}$. As was discussed in the previous section, this might not be the case and therefore one would have to tune the collider to an energy just above the $B_s^*\bar{B}_s^*$ threshold. In such a case, there will be a systematic uncertainty whose magnitude is given by eqs. (53) and (54). Conservatively, the total error can be estimated as the sum of the statistical and the systematic one. Let us remark here that a further increase in the center of mass energy, corresponding to the Υ(6S) mass, for instance, would lead to a considerable decrease in the sensitivity to large values of x_s. In fact, the smallest value of β_{cm} in this case (corresponding to the $B_s^*\bar{B}_s^*$ mode) is given by 0.17, which is equivalent to $[\Delta(t_1-t_2)/\tau]_{syst} > 0.3$.

In fig. 10 we plot the opposite sign dilepton distributions for $x_s = 0, 3, 5, 7$, taking into account the statistical and systematic errors, as well as the mistagging error and the background. Here, the statistical error is taken to be 0.1, and $\sqrt{s}$ is taken to be $2m_{B_s^*}$. In fig. 10a we combine the contributions of the various $B^0\bar{B}^0$ components according to the second model of Byers and Hwang in table 1 [13] (we will refer to

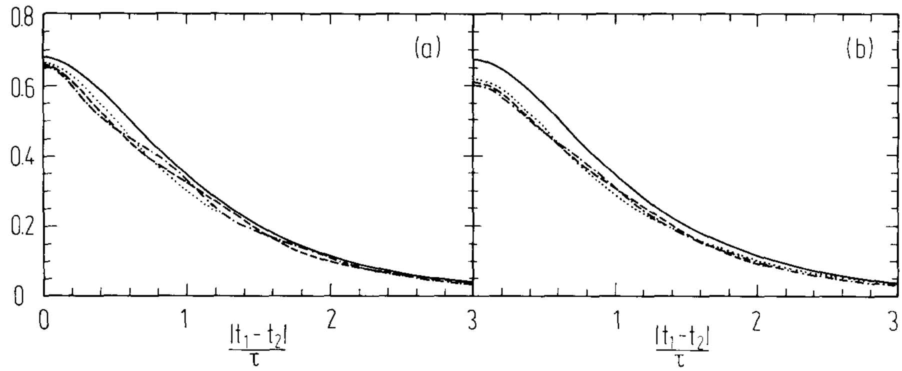

Fig. 10. The opposite sign dilepton distributions, taking into account all discussed effects, as a function of the proper time difference $|t_1 - t_2|/\tau$. A mistagging probability of 5% and $[\Delta(t_1 - t_2)/\tau]_{res} = 0.1$ are assumed, for $x_s = 0$ (solid), 3 (dotted), 5 (dashed), and 7 (dot-dashed): (a) for the scenario BHII, (b) for the equal mixture scenario.

this combination as "BHII"). The charged B^+B^- background is taken to be 1.2 times that due to $B_d\bar{B}_d$ pairs (this is the parameter λ in eq. 10). Similarly, ρ, the ratio of $BB\pi$ to $B_d\bar{B}_d$ initial states (eq. 11), is assumed to be equal to 1. (It might be possible to reduce the value of ρ by detecting charged π's, seeing that they do not come from the decays of either of the two B's, and removing these events from the sample.) As in sect. 3.1, all the distributions are normalized to the total number of dilepton events. In view of the theoretical uncertainties involved in calculating the numbers of BHII, in fig. 10b we consider the extreme case of equal probabilities for B_d and B_s production as well as for the odd and even angular momentum states (this will be referred to as the "equal mixture"). Since the oscillation periods for even-L and odd-L components are equal, the lack of knowledge of their relative weights does not affect the determination of this period. However, the signal due to the modes $B_s\bar{B}_s$ and $B_s\bar{B}_s^* + B_s^*\bar{B}_s$ is considerably reduced due to the Doppler effect. Therefore the measurement of x_s would become difficult unless $B_s^*\bar{B}_s^*$ constituted the dominant contribution. Fortunately, potential models do predict this mode to dominate, for the CM energy just above the threshold for its production. In both figs. 10a and 10b, it is clear that the signal to background ratio becomes very small when all the effects are taken into account. Of course, this gets even worse for larger values of $[\Delta(t_1 - t_2)/\tau]_{res}$.

The small signal to background ratio in the opposite sign dilepton distributions is mainly caused by the large contribution from $B_d\bar{B}_d$, B^+B^-, $B^-B_d\pi^+$, and $B^+\bar{B}_d\pi^-$ initial states. For this reason the oscillation in the same sign dilepton sample provides a better measurement of x_s. In fig. 11, we show the same sign dilepton distribution for $x_s = 0, 3, 5, 10$, for a number of different scenarios. In fig. 11a, we assume no statistical error, but take all other errors into account, using the initial

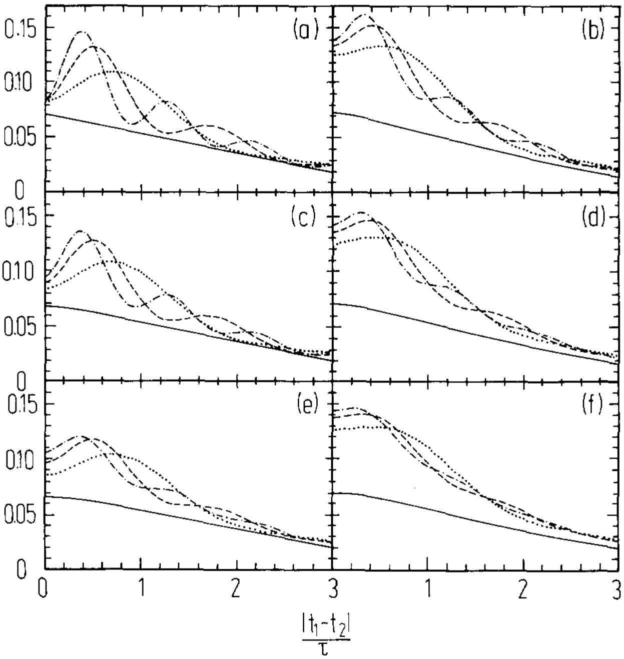

Fig. 11. The same sign dilepton distribution as in fig. 10. The left column is shown assuming the scenario BHII with $[\Delta(t_1 - t_2)/\tau]_{\text{res}} = 0$ (a), 0.1 (c), and 0.2 (e). Similarly, the right column shows the results for the equal mixture scenario (b, d, f). The values of x_s and the curve assignments are the same as in fig. 10.

$B^0\bar{B}^0$ ratios of BHII. Fig. 11b is the same, except that the equal mixture is used. Figs. 11c and 11d use BHII and the equal mixture, respectively, but now for the more realistic value of $[\Delta(t_1 - t_2)/\tau]_{\text{res}} = 0.1$. Finally, the curves with $[\Delta(t_1 - t_2)/\tau]_{\text{res}} = 0.2$ are found in figs. 11e and 11f, again for BHII and the equal mixture, respectively. For a statistical error of 0.1, the oscillations can be seen in both cases, even for the value $x_s = 10$. However, for $[\Delta(t_1 - t_2)/\tau]_{\text{res}} = 0.2$, the signal is almost washed out for the equal mixture. To stress the importance of good vertex resolution, in fig. 12 we plot the same sign dilepton distribution for fixed $x_s = 7$ and four values of the statistical error (0, 0.1, 0.25, 0.5) using the BHII scenario. Although the signal is still clear for 0.1, it is very difficult to see for 0.2, and essentially invisible for a statistical error of 0.5.

In principle, one might expect that, for large statistical errors, the distributions for various x_s would quickly become identical. But, as can be seen in figs. 11e and 11f, this is not the case, especially near $t_1 - t_2 = 0$. However, this effect cannot be used to determine x_s, since the difference depends on the poorly known production probabilities for the various modes. Again, this can be seen from a comparison of figs. 11e and 11f, where we used BHII and the equal mixture, respectively. On the

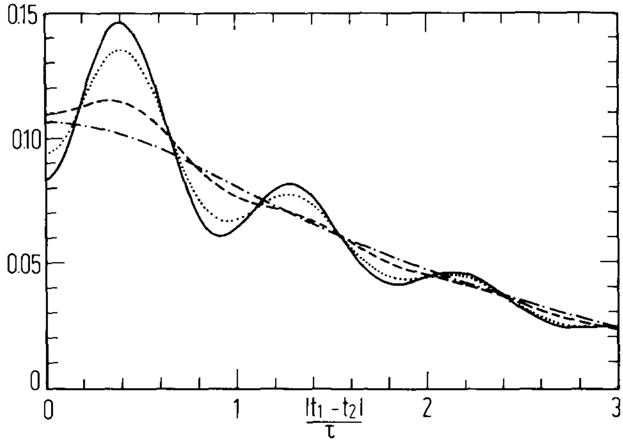

Fig. 12. The same sign dilepton distribution for a fixed value of $x_s = 7$ and $[\Delta(t_1 - t_2)/\tau]_{res} = 0$ (solid), 0.1 (dotted), 0.2 (dashed), and 0.5 (dot-dashed).

other hand, if x_s were known, say from the oscillation length, then measuring the ratio of same sign to opposite sign dilepton rates at $t_1 = t_2$ might provide information on the weights with which the various components contribute. (If $t_1 - t_2 = 0$ were hard to access experimentally, other values could be used, for instance $|t_1 - t_2| = 2\pi/x_s$ as in fig. 6.) This ratio is plotted as a function of $[\Delta(t_1 - t_2)/\tau]_{res}$ in figs. 13a and 13b for $x_s = 0.5$, 3, 5, 10 and 15, using BHII and the equal mixture, respectively. A cautionary remark is in order here. Since only a Monte Carlo simulation can give a reliable estimate of the number of dileptons at $t_1 = t_2$, fig. 13

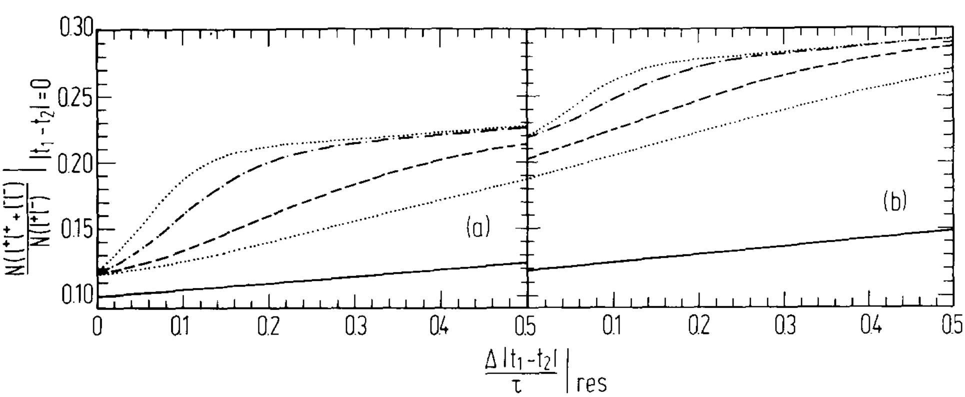

Fig. 13. The ratio of same sign to opposite sign dilepton rates at $|t_1 - t_2| = 0$ as a function of $[\Delta(t_1 - t_2)/\tau]_{res}$ for $x_s = 0.5$ (solid), 3 (dotted), 5 (dashed), 10 (dot-dashed), and 15 (dotted): (a) BHII scenario, (b) equal mixture.

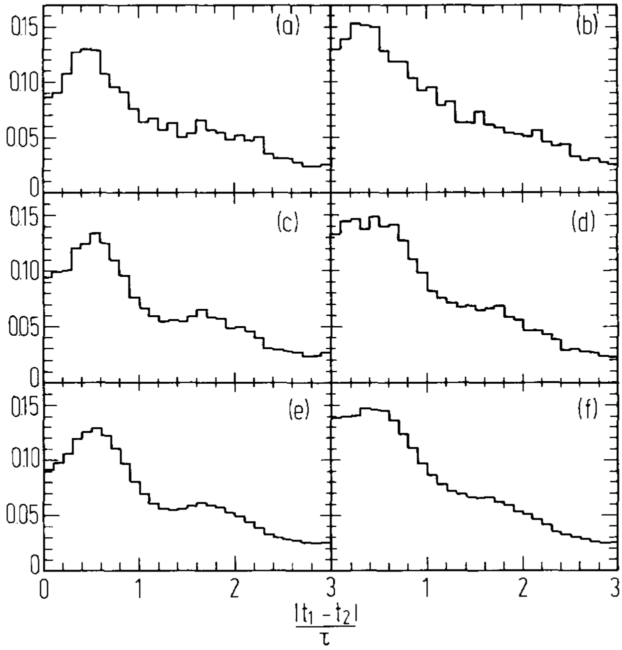

Fig. 14. Simulation of the actual experimental data for the distributions of fig. 11(c) and (d), with $[\Delta(t_1 - t_2)/\tau]_{res} = 0.1$, for $x_s = 5$, and 2×10^4 (a,b), 5×10^4 (c,d), 5×10^5 (e,f), reconstructed dileptons.

can only be regarded as an indication of the effect. On the other hand, for figs. 10–12, the presence of the oscillatory component and its period should be rather insensitive to the smearing procedure employed.

Our final task is to estimate the number of $b\bar{b}$ quark pairs needed to measure x_s at asymmetric colliders. In order to get a reliable number for the statistics required, we generated histograms as in sect. 3.1, assuming the binsize of the experimental distribution to be equal to $[\Delta(t_1 - t_2)/\tau]_{res}$. In fig. 14, we show the histograms for the two scenarios, BHII and the equal mixture, with $[\Delta(t_1 - t_2)/\tau]_{res} = 0.1$ and $x_s = 5$. Each case is presented for three different numbers of detected same sign dilepton events, 2×10^4, 5×10^4, and 5×10^5. Taking into account semileptonic branching ratios, which give a factor $1/(0.24)^2$, and allowing for both finite experimental efficiency and the fact that some of the signal goes down the beam pipe (an estimated combined factor of 8), these correspond to about 2×10^6, 5×10^6, and 5×10^7 initial $b\bar{b}$ quark pairs, respectively. For both the BHII and the equal mixture scenarios, the period can probably be measured with about 5×10^4 same sign dilepton events. Fig. 15 shows similar histograms, but for $x_s = 10$. Here, although the signal can be seen in the BHII scenario with only 5×10^4 events, it cannot be seen for the more pessimistic equal mixture, even with 5×10^5 events.

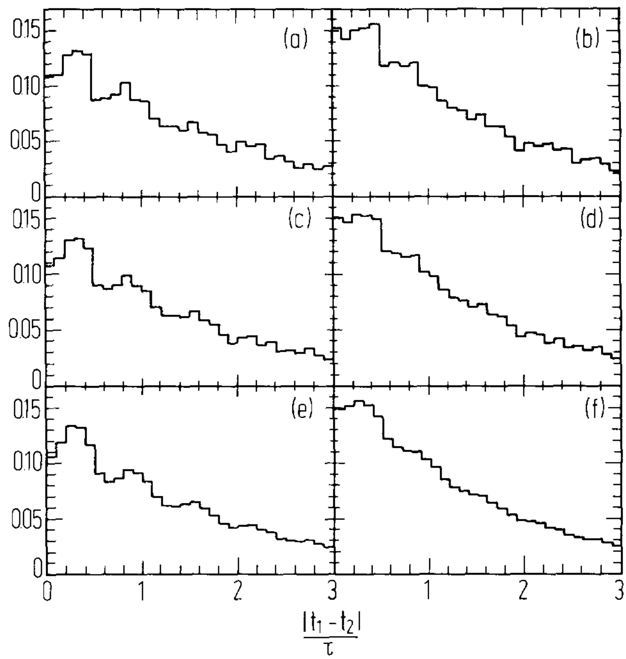

Fig. 15. As in fig. 14, but now for $x_s = 10$.

With 5×10^4 events, for the equal mixture, the maximum value of x_s which can be obtained is about 7. The histograms for $x_s = 3$ and 5×10^4 events are shown in fig. 16. In both cases it might be possible to extract x_s by assuming that all modes except $B_s^* \bar{B}_s^*$ contribute a pure exponential, and then doing a 2-parameter fit to the distribution. We further emphasize the importance of good vertex resolution in fig. 17. Here the histograms are plotted for $x_s = 5$, but $[\Delta(t_1 - t_2)/\tau]_{res} = 0.2$. By

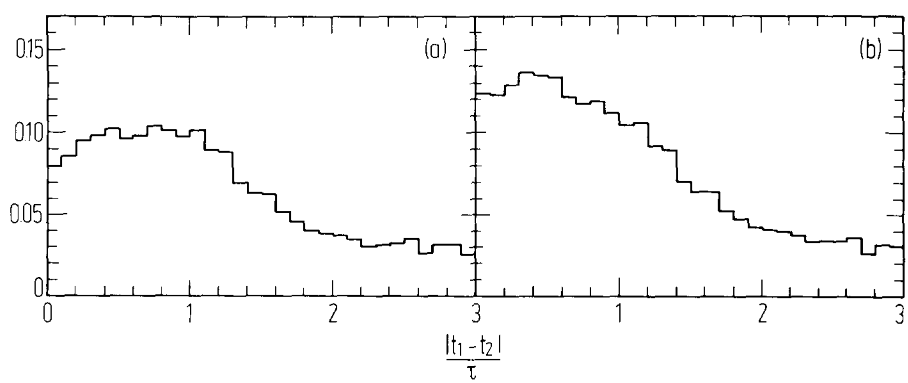

Fig. 16. As in fig. 14(c, d), but now for $x_s = 3$.

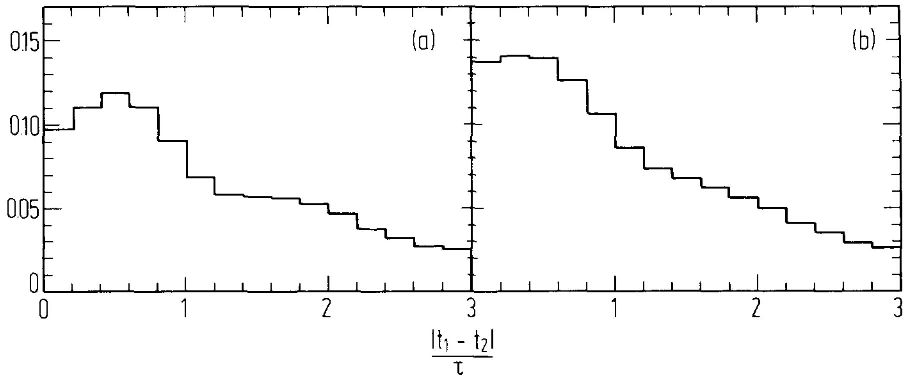

Fig. 17. As in fig. 14(e, f), but now for $[\Delta(t_1 - t_2)/\tau]_{res} = 0.2$.

comparison with fig. 14, it is clear that x_s cannot be extracted from these distributions. We therefore conclude that, in addition to at least 5×10^6 $b\bar{b}$'s, a vertex resolution $\Delta l = 25$ μm or better is necessary. However, the largest value of x_s which can be measured is about 10. Of course, the precise upper limit depends strongly on the actual production ratios of the various initial states.

Finally, one might hope that an additional D_s tag, which would have the effect of dramatically reducing the background, would lead to the requirement of a smaller number of $b\bar{b}$ quark pairs for the determination of x_s. However, the poor efficiency of D_s detection outweighs the gain in the signal to background ratio. A detailed analysis shows that at least one order of magnitude increase in statistics is unavoidable, with only a marginal gain in the largest value of x_s measurable.

4. Conclusions

In the standard model, x_s is expected to be at least 3. Its value can, in principle, be obtained using time integrated or time dependent means. We have analysed both methods in detail, focussing on (i) the number of $b\bar{b}$ quark pairs needed, (ii) the range of x_s accessible, and (iii) the physics assumptions upon which each method is dependent.

There are two possibilities for time integrated methods. First of all, the experiment can be performed at an energy around the mass of the $\Upsilon(5S)$. In this case x_s is extracted from a measurement of the ratio of same sign to opposite sign dileptons. In order to enhance the number of B_s's in the sample, an additional tag on a D_s is required. We estimate that 2×10^8 $b\bar{b}$ pairs are required to determine R_s to 8%. However, this is crucially dependent on the assumption that the fraction of $B_s^0\bar{B}_s^0$ pairs in one orbital angular momentum state (i.e. either even or odd) is negligible. If this is not the case, the inability to accurately measure $\hat{s}_o/\hat{s}_e$ will make it impossible to determine R_s with sufficient precision to test the standard model.

Time integrated techniques can also be used at energies high above the Υ(5S) mass. In this case we require that the initial state be $B_s^0 B^-$ (or $\overline{B}_s^0 B^+$), that the charged B be fully reconstructed, and that the B_s be identified through its semi-leptonic decay mode $B_s \to \ell D_s X$. r_s is then obtained from $N(\ell^+ B^+ + \ell^- B^-)/N(\ell^+ B^- + \ell^- B^+)$. Assuming that the background can be reduced to less than 5%, and that the ratios of production probabilities p_d/p_s and p_{ch}/p_s can be determined to at least 25%, we estimate that r_s can be measured to 8% with 3–7×10^8 $b\bar{b}$ pairs.

For both of these time integrated methods, a measurement of R_s (or r_s) to 8% corresponds (in the most optimistic case) to x_s in the range $3 \leqslant x_s \leqslant 10$ at the 1σ level. Realistically, however, it seems very unlikely that either of these methods will yield constraints on x_s at the 90% c.l. better than those provided by x_d and our knowledge of the CKM matrix. Should x_s turn out to be smaller than predicted by the standard model, these techniques could be quite useful. However, we feel that, for a standard model value of x_s, time integrated methods are not likely to provide more information.

Time dependent methods are much more promising. As in the time integrated case, there are two possibilities for such experiments. First, the time dependence of B_s oscillations can be examined at energies high above the $B_s^0 \overline{B}_s^0$ production threshold. In this case, the decay of a B_s meson is identified, and the time of its decay measured. The charge of the lepton in a semi-leptonic decay determines whether the other B contained a b or a $\bar{b}$ quark when it decayed. $N(B_s^0 \overline{B} + \overline{B}_s^0 B)$ (or $N(B_s^0 B + \overline{B}_s^0 \overline{B})$) is then plotted vs. t, and x_s is obtained from the period of oscillation of the curve. However, the time of the decay is not determined directly – it must be obtained from a measurement of the energy of the B_s and the distance of flight. Assuming that both are measured accurately enough that $\Delta t/\tau$ can be determined to 10%, we find that at least 3×10^8 $b\bar{b}$ quark pairs are needed. With this method, a value of x_s up to about 15 is accessible. On the other hand, if $\Delta t/\tau$ can only be measured to 25%, the oscillations are essentially washed out.

The other possibility for a time dependent determination of x_s is to use an asymmetric e^+e^- collider and to run the experiment near the Υ(5S). Here, although it is not possible to measure the decay time of an individual B_s, the time difference between the decays of two B's is experimentally accessible. With this technique, x_s can be obtained by simply looking at oscillations in the number of same sign (or opposite sign) dileptons as a function of this time difference. We find that it is best to look at the same sign dilepton distribution. Since the detection of a D_s meson is not necessary, a reduction in the number of $b\bar{b}$ pairs required is expected. Assuming that the vertex resolution is at least 25 μm (which corresponds to $\Delta(t_1 - t_2)/\tau = 0.1$), a value of x_s up to about 10 can be measured with 5×10^6 $b\bar{b}$ pairs. However, the range of x_s accessible is quite dependent on the actual production rates of the individual states. For instance, for the pessimistic case of an equal mixture of initial states ($B_d^0 \overline{B}_d^0$ and $B_s^0 \overline{B}_s^0$ pairs in both even and odd orbital angular momentum states), the maximum value of x_s which can be obtained with 5×10^6 $b\bar{b}$'s is about 7. Furthermore, if the vertex resolution is only 50 μm, the oscillations cannot be seen at all.

From this study, it is likely that time dependent methods are needed, for standard model values of x_s. Experiments which run at energies high above the $B_s^0\bar{B}_s^0$ threshold can measure x_s in the range 3–15, but require at least 3×10^8 $b\bar{b}$ quark pairs. Asymmetric colliders near the $\Upsilon(5S)$ can perform this measurement with fewer ($\sim 5 \times 10^6$) $b\bar{b}$ pairs, but are only sensitive to values of x_s up to about 10 (with this number of $b\bar{b}$'s). Work has already been done investigating the feasibility of both of these machines for the examination of *CP* violation in the B system. In light of the fact that the measurement of x_s is a very important test for the standard model, we strongly encourage that these efforts continue.

We thank R. Peccei and H. Schröder for helpful discussions and a critical reading of the manuscript. We thank T. Nakada for useful conversations, and for the results of his Monte Carlo simulation. Discussions with A. Ali, D. Cassel and G. Feldman were also of great help. We are grateful to G. Ingelman for the JETSET program. P.K. thanks M. Pawlak for helpful conversations. D.L. wishes to thank D. Hitlin, M. Witherell, A. Sanda, and P. Patel for helpful discussions, and the organizers of Snowmass '88, where some of this work was done. H.S. would like to thank *Acciones Intgradas* and the theory group of the Univ. Autònoma de Barcelona, where part of this work was done.

Appendix

In this appendix we present the ingredients needed to calculate time dependent distributions folded with a gaussian error factor. These distributions are linear combinations of terms of the following form

$$D(v) = \frac{1}{\sigma\sqrt{2\pi}} \int_{-\infty}^{\infty} g(v')\exp\left[-\frac{(v-v')^2}{2\sigma^2}\right] dv', \qquad (A.1)$$

where σ is the experimental resolution. For oscillations high above the $B_s^0\bar{B}_s^0$ threshold (sect. 3.1), the function of $g(v)$ is one of

$$\theta(v)e^{-v}, \qquad \theta(v)e^{-v}\cos xv, \qquad \theta(v)e^{-v}\sin xv, \qquad (A.2)$$

where $v = t/\tau$ and $\theta(v)$ is the step function. (As can be seen from eq. (45), the function $\theta(v)e^{-v}\sin xv$ is not necessary, but has been included here for completeness.) For the case of oscillations near the $B_s^0\bar{B}_s^0$ threshold (sect. 3.2), $v = (t_1 - t_2)/\tau$, and $g(v)$ is one of

$$e^{-v}, \qquad e^{-v}\cos sv, \qquad e^{-v}\sin xv. \qquad (A.3)$$

A straightforward calculation yields the following results for $D(v)$ with $g(v)$ as given in eq. (A.2):

$$D(v)=\begin{cases}\operatorname{Re}H_1(v)|_{x=0}, & \text{for } g(v) \text{ purely exponential},\\ \operatorname{Re}H_1(v), & \text{for } g(v)\propto\cos xv,\\ \operatorname{Im}H_1(v), & \text{for } g(v)\propto\sin xv.\end{cases} \tag{A.4}$$

For $g(v)$ as given in eq. (A.3),

$$D(v)=\begin{cases}\operatorname{Re}(H_1(v)+H_2(v))|_{x=0}, & \text{for } g(v) \text{ purely exponential},\\ \operatorname{Re}(H_1(v)+H_2(v)), & \text{for } g(v)\propto\cos xv,\\ \operatorname{Im}(H_1(v)+H_2(v)). & \text{for } g(v)\propto\sin xv.\end{cases} \tag{A.5}$$

The functions $H_1(v)$ and $H_2(v)$ in the above equations are defined as follows:

$$\left.\begin{matrix}H_1(v)\\ H_2(v)\end{matrix}\right\}=\tfrac{1}{2}\left\{\exp\left[\tfrac{1}{2}\sigma^2(1-ix)^2\mp v(1-ix)\right]\right\}\left[1-\operatorname{erf}\left(\frac{\sigma^2\mp v}{\sqrt{2}\,\sigma}-i\frac{x\sigma}{\sqrt{2}}\right)\right], \tag{A.6}$$

where $\operatorname{erf}(z)$ is the error function (of complex argument) [30].

References

[1] ARGUS Collab., H. Albrecht et al., Phys. Lett. B192 (1987) 245

[2] CLEO Collab., A. Jawahery, Proc. XXIVth Int. Conf. on High Energy Physics, Munich, 1988

[3] A. Ali, DESY preprint DESY 87-083 (1987);
J. Donoghue, T. Nakada, E. Paschos and D. Wyler, Phys. Lett. B195 (1987) 285;
J. Ellis, J. Hagelin and S. Rudaz, Phys. Lett. B192 (1987) 201;
I.I. Bigi and A.I. Sanda, Phys. Lett. B194 (1987) 307;
J. Maalampi and M. Roos, Phys. Lett. B195 (1987) 489;
V. Barger, T. Han, D.V. Nanopoulos and R.J.N. Phillips, Phys. Lett. B194 (1987) 312;
H. Harari and Y. Nir, Phys. Lett. B195 (1987) 586;
Y. Nir, SLAC preprint SLAC-PUB-4368 (1987);
V.A. Khoze and N.G. Uraltsev, Leningrad preprint 1290 (1987);
G. Altarelli and P. Franzini, Z. Phys. C37 (1988) 271;
W.A. Kaufman, H. Steger and Y.P. Yao, Univ. of Michigan preprint UM-TH-87-13, (1987)

[4] P. Krawczyk, H. Steger, D. London and R. Peccei, Nucl. Phys. B307 (1988) 19

[5] G. Altarelli and P. Franzini, Z. Phys. C37 (1988) 271

[6] LEP Design Report, CERN-LEP/84-01 (1984)

[7] C.Y. Prescott, SLAC preprint SLAC-PUB-2854 (1981); Proc. of the SLC Workshop, SLAC-247 (1982)

[8] PSI preprint PR-88-09 (1988)

[9] A. Ali et al., Proc. of the HERA Workshop, ed. R.D. Peccei (DESY, Hamburg, 1988) p. 395

[10] K. Hagiwara, KEK preprint KEK-TH-170 (1987)

[11] A. Pais and S.B. Treiman, Phys. Rev. D12 (1975) 2744

[12] A.J. Buras, W. Slominski and H. Steger, Nucl. Phys. B238 (1984) 529; B245 (1984) 369;
J. Hagelin, Nucl. Phys. B193 (1981) 123

[13] N. Byers and D.S. Hwang, Proc. of the Workshop on High Sensitivity Beauty Physics at Fermilab, ed. A.J. Slaughter, N. Lockyer and M.P. Schmidt (Fermi National Accelerator Laboratory, Batavia, 1987) p. 199
[14] J. Lee-Franzini, SUNY preprint Print-88-0457 (Stony Brook) (1988)
[15] A.D. Martin and C.-K. Ng, Z. Phys. C40 (1988) 133;
S. Ono, A.I. Sanda and N.A. Törnqvist, Phys. Rev. D38 (1988) 1619
[16] CLEO Collab., D. Besson et al., Phys. Rev. Lett. 54 (1985) 381
[17] P. Krawczyk and H. Steger, in preparation
[18] ARGUS Collab., R. Ammar et al., Proc. of the Int. Eurphys. Conf. on High Energy Physics, ed. O. Botner (Uppsala Univ., Uppsala, 1987) p. 360
[19] M. Bauer, B. Stech and M. Wirbel, Z. Phys. C34 (1987) 103
[20] Particle Data Group, M. Aguilar-Benitez et al., Phys. Lett. B170 (1986) 1
[21] T. Nakada at Snowmass '88
[22] ARGUS Collab., H. Albrecht et al., Phys. Lett. B197 (1987) 452
[23] T. Sjöstrand and M. Bengtsson, Comp. Phys. Comm. 43 (1987) 367
[24] T. Nakada, private communication
[25] A. Ali and F. Barreiro, Z. Phys. C30 (1986) 635
[26] W.B. Atwood, I. Dunietz and P. Grosse-Wiesmann, SLAC preprint SLAC-PUB-4544 (1988)
[27] R. Aleksan, J.E. Bartelt, P. Burchat and A. Seiden, SLAC preprint SLAC-PUB-4673 (1988)
[28] P. Patel and H. Schröder, private communication
[29] G. Feldman at Snowmass '88
[30] M. Abramowitz and I.A. Stegun, eds., Handbook of mathematical functions (National Bureau of Standards, 1964)